

More than 20 Years of Experience Using the Large Wave Flume (GWK) – Selected Research Projects

By HOCINE OUMERACI

Z u s a m m e n f a s s u n g

Nach einer einführenden Betrachtung über Maßstabeffekte und die Notwendigkeit großer Versuchseinrichtungen sowie nach einer kurzen Beschreibung des Großen Wellenkanals (GWK) des Forschungszentrums Küste (FZK), einer gemeinsamen zentralen Einrichtung der Leibniz Universität Hannover und der Technischen Universität Braunschweig, wird kurz auf die Expertise des Autors und seiner Forschungsgruppe bei der Nutzung des GWK eingegangen. Zur Illustration werden im Hauptteil des Beitrages ausgewählte Projektbeispiele aufgeführt, die unter der Leitung des Autors durchgeführt wurden. Hierzu zählen u.a. (i) Seegangbelastung und Standsicherheit von Deckwerken sowie deren Baugrund, (ii) Druckschlagbelastung und dynamische Antwort von Caisson-Bauwerken sowie deren Baugrund durch brechende Wellen, (iii) hydraulische Wirksamkeit wellendämpfender Bauwerke im Küstenschutz/Hafenbau mit besonderem Fokus auf nicht herkömmliche Bauwerke, (iv) seeganginduzierte Filterströmungen in geschütteten Bauwerken, (v) Stabilität von Bauwerken aus geotextilen Sandcontainern, (vi) Seegangbelastung, Wellenüberlauf, Standsicherheit und Bruch von Seedeichen, (vii) Einfluss von Wellenbrechern auf schlanke Pfähle im Tief-/Flachwasser, (viii) seeganginduzierter Kolk um Bauwerke sowie Kolkchutzmaßnahmen und (ix) küstennaher Sedimenttransport und Strand-/Dünenerosion durch extreme Sturmfluten.

S c h l a g w ö r t e r

Großer Wellenkanal (GWK), Maßstabeffekte, Seegangbelastung, Druckschlagbelastung, brechende Wellen, Wellenüberlauf, Porenwasserdrücke, Baugrundstabilität, Küstenschutzbauwerke, Wellenbrecher, Seedeiche, Deckwerke, Offshore-Bauwerke, geotextile Sandcontainer, Kolk um Seebauwerke, Kolkchutz, küstennahe Sedimentdynamik, Strand- und Dünenerosion

S u m m a r y

This paper discusses scale effects in physical hydraulic models, illustrating the necessity of large-scale experimental facilities. A brief description is given of the Large Wave Flume (GWK), which is a key facility of the Coastal Research Centre (FZK) jointly established by the Leibniz Universität Hannover and the Technische Universität Braunschweig. The primary expertise of the author and his research team is also briefly outlined. The latter is demonstrated by selected projects carried out in the GWK under the direction and supervision of the author. These include among others (i) Wave loading and the response of porous bonded revetments, including the response of their foundations, (ii) Wave loading and the dynamic response of caisson breakwater foundations, (iii) Hydraulic performance of wave damping structures with particular emphasis on non-conventional structures, (iv) Wave-induced porous flow in rubble mound structures, (v) Hydraulic stability/performance of coastal structures made of geotextiles, (vi) Effect of wave overtopping and breaching of sea dikes, (vii) Breaking-wave impact on slender pile structures in deep/shallow water, (viii) Wave-induced scour around marine structures and scour protection, (ix) Nearshore sediment dynamics and beach/dune profile development under extreme storm surge conditions.

Keywords

Large Wave Flume (GWK), scale effects, wave loading, impact loads, breaking waves, wave overtopping, pore pressure, soil foundation stability, coastal structures, breakwaters, sea dikes, dike breaching, wave-induced porous flow, geotextile sand containers, revetments, offshore structures, scour around marine structures, scour protection, nearshore sediment dynamics, beach/dune erosion

Contents

1. Introduction	181
2. Necessity of large wave facilities and the Large Wave Flume (GWK)	182
2.1 Scale effects and the necessity of large-scale wave facilities	182
2.2 Large Wave Flume research facility of the Coastal Research Centre (FZK): a Brief Description	185
2.3 Primary expertise and experience using the Large Wave Flume in brief	187
3. Outline of selected research projects performed in the Large Wave Flume (GWK)	190
3.1 Wave loading and the response of a PBA revetment	190
3.2 Wave loading and the response of a caisson breakwater foundation	198
3.3 Hydraulic performance of wave damping structures	203
3.4 Wave-induced flow on and within rubble mound breakwaters	213
3.5 Hydraulic stability/performance of coastal protection structures made of geotextiles	217
3.6 Effect of wave overtopping and breaching of sea dikes	220
3.7 Breaking-wave impact on slender pile structures	224
3.8 Wave-induced scour around marine structures and scour protection	227
3.9 Sediment dynamics and beach/dune profile development under extreme storm surge conditions	230
4. Concluding remarks and perspectives	234
5. Acknowledgements	234
6. References	235

1. Introduction

This paper originates from the extended contents of a keynote lecture held at a workshop in Tainan/Taiwan by the author on December 10, 2010 to commemorate the 60th Anniversary of the Tainan Hydraulic Laboratory (THL). As the latter has a large wave flume similar to the GWK, the author was invited to report on his own experiences using such large-scale wave facilities over more than two decades. This paper therefore primarily aims at providing an outline of selected research projects which were performed under the scientific supervision of the author using the Large Wave Flume (GWK) of the Coastal Research Centre (FZK), a joint institution of the Leibniz Universität Hannover and the Technische Universität Braunschweig/Germany, in order to illustrate the capabilities of similar large-scale testing facilities and their increasing importance, especially in view of their pivotal role in modelling complex processes and interactions in the context of the expected increase of storm surge events due to the impact of climate change in coastal zones.

Firstly, a brief review is given of the necessity of large wave facilities such as the GWK to avoid/reduce scale effects and their importance for studying very complex interactions between waves and natural barriers, man-made structures and the seabed. This is followed by a brief description of the GWK.

The major part of this paper is dedicated to a brief description of a few selected examples among the research projects performed in the GWK under the supervision of the author to illustrate the capabilities and possible applications of similar large-scale facilities. Considering the primary aim of this paper, the description of each project is documented as briefly as possible. References for more detailed descriptions are also provided. Because the primary interest of the author is focussed on modelling the interaction between sea waves, man-made structures/natural barriers and the seabed, the examples outlined in Section 3 are selected accordingly. The research interests of the author include (i) breaking-wave impact loading and the response of revetments and their foundations, (ii) wave loading and the response of the foundations of gravity structures under extreme wave conditions, (iii) hydraulic performance of wave-damping structures, with particular emphasis on non-conventional structures, (iv) wave-induced flow on and within rubble mound breakwaters and structures, (v) hydraulic stability/performance of marine structures made of geotextile sand containers (GSC), (vi) effect of wave overtopping and breaching of sea dike /coastal barriers induced by wave impact/overtopping, (viii) breaking-wave impact load on slender pile structures, (ix) wave-induced scour around marine structures and (x) sediment transport in the surf zone and beach/dune profile development under extreme storm surge conditions.

Finally, several remarks are also included regarding the necessity of large-scale facilities for investigating hydrodynamic processes and their interactions with structures and the seabed, which cannot be studied properly in small-scale models due to the scale effects associated with energy dissipation and other mechanisms. The increasing role of large-scale testing facilities is also highlighted in view of the promising future of composite modelling. In order to reduce both laboratory effects and scale effects in the modelling of coastal hydrodynamic and morphodynamic processes, the need for much larger wave basins than existing basins worldwide is also underlined.

2. Necessity of large wave facilities and the Large Wave Flume (GWK)

2.1 Scale effects and the necessity of large-scale wave facilities

Although physical modelling is and will always remain a powerful research and design tool (OUMERACI, 1999), it also has a number of limitations, among which scale and laboratory effects are certainly the most important (OUMERACI, 1984; HUGHES, 1993; KORTENHAUS and OUMERACI, 2003; OUMERACI et al., 2001b). In order to primarily overcome scale effects in coastal/oceanographic engineering applications, large wave facilities such as those illustrated in Fig. 1 have emerged in recent decades. In order to underline the importance of such large facilities, a very brief overview of scale effects is provided below.

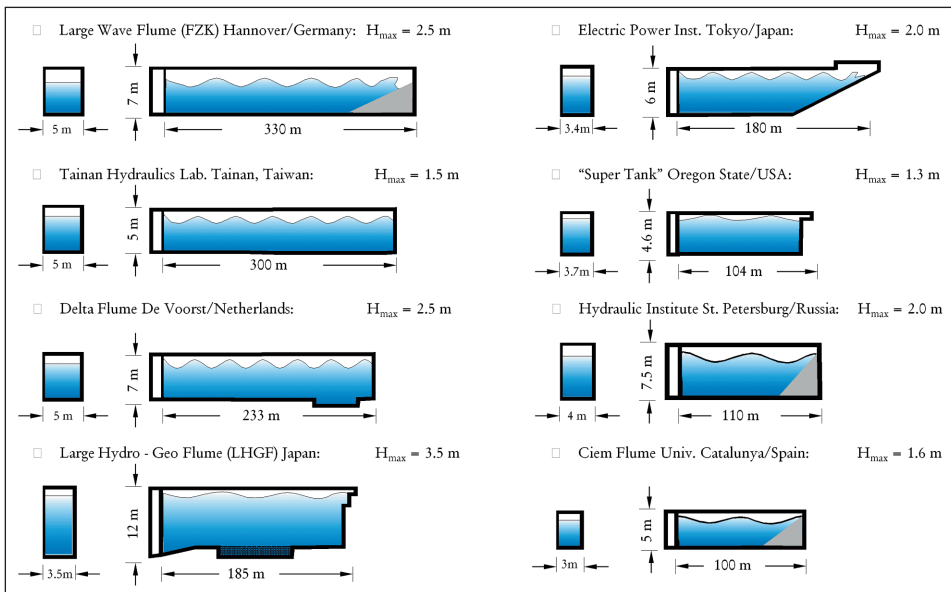


Fig. 1: The world's largest wave flume facilities for coastal engineering applications

In contrast to laboratory effects, which have nothing to do with similarity laws such as Froude's law and Reynolds' law, scale effects arise from the inability of a scale model to reproduce all relevant forces of the prototype by fulfilling the related similarity laws. In fact, laboratory effects are solely due to the inappropriate representation of the forcing functions and the boundary conditions in the model, i.e. they arise from the inability of the model to correctly reproduce the driving forces such as waves, currents, etc., under laboratory conditions as well as from solid boundaries such as wave paddles, side walls, etc., which do not exist as such in the prototype. Because laboratory effects also exist in large-scale models, a considerable amount of efforts is still required to improve our understanding of these effects and reduce their influence, despite the relatively recent developments in wave generation and active wave absorption techniques.

Because wave motion is primarily governed by gravity forces, most scale models in coastal engineering are run according to Froude's law of similitude, i.e. all other forces such as friction, elasticity and surface tension are neglected, even though these might be considerably exaggerated in the model. The errors which may result from these exaggerations and dissimilarities are called scale effects, i.e. they always occur in scale models, but rapidly decrease when the size of the model approaches the prototype scale (Fig. 2).

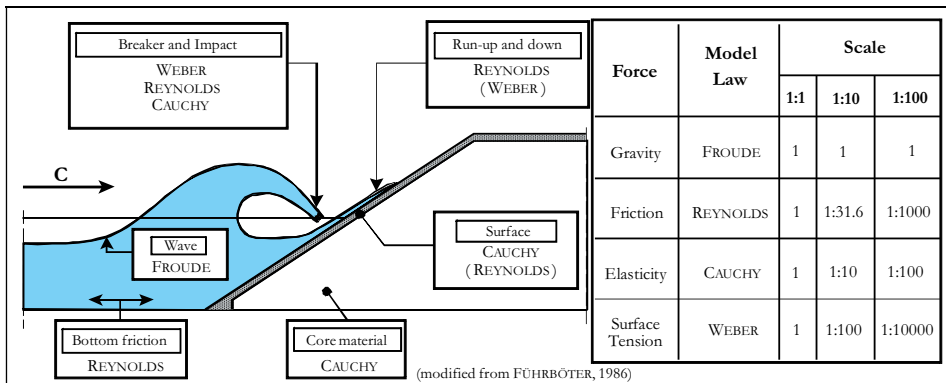


Fig. 2: Scale effects in modelling wave loading and the response of sea dikes (modified from FÜHRBÖTER, 1986)

In order to discuss scale effects in coastal hydraulic models it is necessary to distinguish between short and long wave models as well as between structure and sediment transport models (OUMERACI, 1984; 1994a; 1999; 2010c). In contrast to long wave models and tidal models, which are generally distorted, short wave models cannot be distorted.

The following discussion is restricted to a brief review of scale effects. Further details and references are given by OUMERACI (1984) and HUGHES (1993). For short wave models, most of the scale effects originate from the dissimilarity of bottom friction and wave transmission through porous structures. Surface tension effects may also be important if the wave period is less than $T = 0.35$ s and the water depth is less than $h = 2$ cm. The viscous and bottom effects may be assessed and corrected by existing formulae (HUGHES, 1993). Scale effects in wave transmission can be reduced by using the nomograms provided by LE MEHAUTÉ (1965) for both long and short waves.

For long wave models the above considerations on the effects of surface tension and bottom friction are also valid for undistorted models. Additional scale effects occur with regard to wave reflection, refraction, diffraction, and harbour resonance phenomena, while scale effects in wave transmission still remain appreciable (OUMERACI, 1984).

For structure models, which are generally used to simulate wave loading and the response behaviour and stability of coastal and offshore structures, the above mentioned considerations for short wave models are also valid in principle. Moreover, scale effects depend greatly on the type of structure investigated (rubble-mound structures, vertical breakwaters, etc.) as well as on the objective of the study (wave loading, stability, etc.).

In the case of rubble mound breakwaters, the most critical scale effects are mainly due to the dissimilarity of the flow field within the breakwater core because in the most com-

monly used small-scale models, viscous effects dominate (Reynolds number related to the grain size of core material of less than $Re = 3 \cdot 10^4$). This also significantly affects several other processes such as the uplift pressure on crown walls, wave run-up and overtopping, wave transmission and reflection, and possibly also wave-induced forces on the armour units.

In the case of vertical breakwaters and similar monolithic structures subject to breaking waves, the most serious scale effects arise from an incorrect reproduction of the impact load, mainly due to the dissimilarity of air entrainment/entrapment in the breaker. Although methods have been suggested for correcting such effects (e.g. OUMERACI et al., 2001b), large-scale model testing close to the prototype scale still remains the best alternative.

For sediment transport models such as those used to study beach and dune profile changes during storm surges, scour in front of coastal structure, etc., it has been shown that quantitative results can hardly be obtained from the commonly used small-scale models because the four similitude criteria as described by OUMERACI (1984; 1994a; 2010c) can never be fulfilled simultaneously. Here again, the best alternative is the use of scale models approaching the prototype scale.

The adopted research strategy, which combines field observations, analytical and numerical modelling as well as small and large-scale model testing, is outlined in Fig. 3. The figure also indicates the central role of the latter in the overall research strategy and the ultimate scientific result, which concerns the development of generic conceptual models based on a physical understanding of the most relevant processes and their interactions.

It should also be mentioned that a research strategy directed towards “Composite Modelling” is already emerging (OUMERACI, 1999; 2010c). The idea to overcome the drawbacks of physical and numerical modelling by combining the strengths of both physical and numerical models first led to the commonly known “Hybrid Modelling”. A few decades later, “Composite Modelling” has emerged. This is more generic and more flexible in the sense that it combines not only physical and numerical models in a basically different manner, but may also include analytical, semi-analytical and empirical models, and field measurements, provided these contribute to the construction of validated process models (OUMERACI, 1999; 2010c). Even the results of hybrid models can be incorporated. The most important thing is that the prospective results of Composite Modelling should (i) be much more generic than other results from physical, numerical or hybrid modelling, (ii) go beyond echoing the equations involved in numerical and hybrid models and (iii) be obtainable at far lower cost and more quickly than from conventional complex models, including many processes and interactions. The principle of Composite Modelling consists in subdividing a very complex and problem into several simple and more easily tractable processes. The latter should be described by the most appropriate methods in order to obtain the most reliable process models possible, including physical and validated numerical and analytical models. An important implication of the advent of Composite Modelling is that the two following trends will be encouraged to a greater extent in the future: (i) the development of large-scale testing facilities to reduce scale effects and (ii) the development of improved techniques to reduce laboratory effects (e.g. active and passive wave absorption techniques).

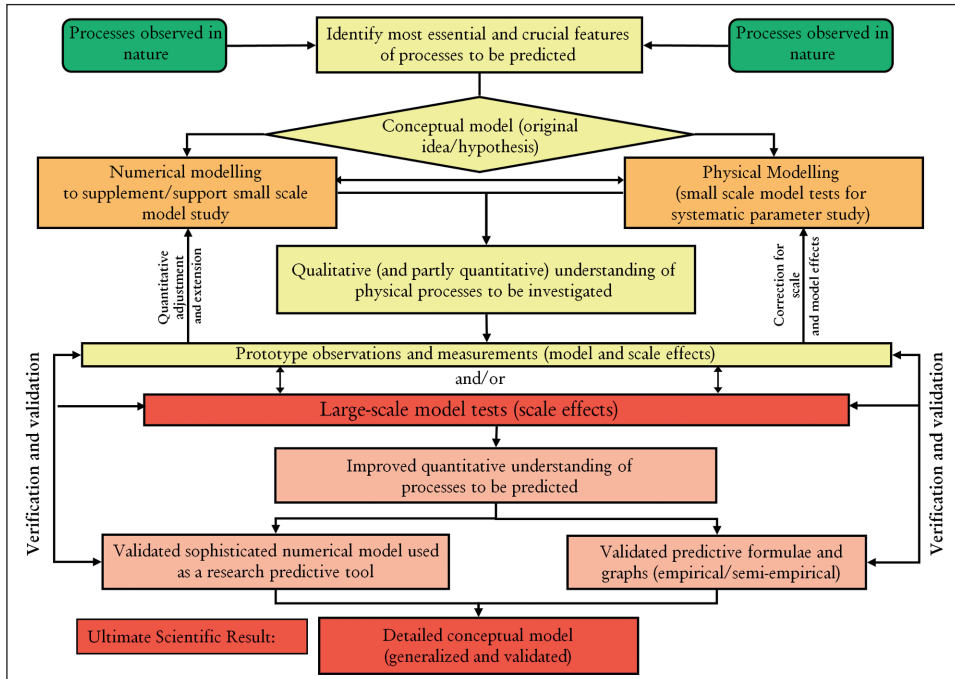


Fig. 3: Role of large-scale model testing within the framework of a basic research strategy

2.2 Large Wave Flume research facility of the Coastal Research Centre (FZK): a Brief Description

The Large Wave Flume (GWK) in Hanover, which was completed in 1983 and financed by the German Research Council (DFG), constitutes the main wave facility of the Coastal Research Centre (FZK) jointly administered and operated by the Leibniz Universität Hannover and the Technische Universität Braunschweig. The flume has an effective length of 307 m, a depth of 7 m and a width of 5 m (Fig. 4). More details of the wave flume itself and historical background information are provided by GRÜNE and FÜHRBÖTER (1975), SPARBOOM (1988) and FÜHRBÖTER et al. (1989). Further details of the FZK are given by OUMERACI (1998). Further information, including procedures for operating the GWK, may be found on the website of the FZK: <http://www.fzk-nth.de/494.html>.

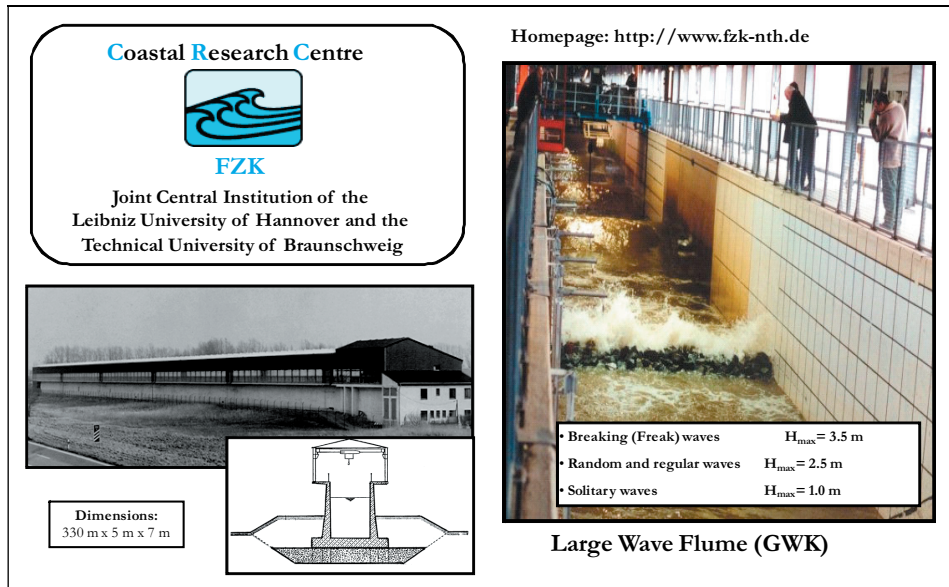


Fig. 4: Large Wave Flume (GWK): (a) general view and cross-section,
(b) waves generated during a test run

Fig. 1 illustrates the largest wave flumes currently used in various countries for carrying out coastal/ocean engineering research. The GWK in Hanover continues to be the largest wave flume worldwide.

Different types of waves can be generated by a piston-type wave generator with an upper flap and a power rating of 900 kW. A maximum stroke of ± 2.0 m of the paddle (max. velocity $v \approx 1.7$ m/s and max. acceleration $a = 2.1$ m/s²) combined with upper flap movements of ± 10 degree of the flap can be achieved. Regular waves with heights of up to about 2.0 m and with periods of up to $T = 10$ s can be generated in water depths of up to 5 m. In the case of irregular waves (PM, JONSWAP, TMA spectra), it is possible to realise significant wave heights of up to $H_{s,\max} = 1.4$ m with peak periods of up to $T_p = 8.0$ s, whereas for solitary waves, significant wave heights of up to $H_{\max} = 1.10$ m are attainable. Single breaking waves in deep water using Gaussian wave packets of more than 3.0 m in height can also be generated (wave focussing). An online wave absorption control system permits the generation of wave trains unaffected by re-reflection at the paddle over almost any time duration.

The measuring techniques available include, among others, (i) wave gauges (>20), (ii) 1-D, 2-D and 3-D current meters (>15), (iii) pressure transducers (>75) with a pressure range of 0.7–10 bar, (iv) displacement meters and accelerometers, (v) wave runup step gauges, (vi) integrated weighting systems for wave overtopping, (vii) optical back-scattering sensors (OBS) and acoustic back-scattering sensors (ABS) to measure vertical profiles of suspended sediment concentration, (viii) a computer-controlled bottom profiler to automatically monitor morphological changes as well as video and underwater cameras. A movable carriage on which the bottom profiler and other instruments can be mounted permits measurements at any location along the flume during tests. More recently, a high-resolution multi-beam sonar system has been deployed to investigate the 3-D development of seabed scour around a pile structure for offshore wind turbines (see Section 3.8).

Before commencing with the construction of large-scale models in the GWK, numerical modelling and/or smaller-scale tests are generally performed in small or medium-size wave flumes in order to identify expected problems/difficulties as well as to optimise the locations/numbers of the measuring/observation devices and the testing programme in the GWK. Such preliminary tests are also often applied to assess and correct possible scale effects. For this purpose and in order to achieve better visualisation/improved observations of the processes which are simultaneously measured, smaller wave flumes such as the twin-wave flumes of the Leichtweiß-Institute (Fig. 5) were often used. The latter medium-size wave facility is also unique in the sense that identical wave conditions can be generated simultaneously or independently in both flumes.

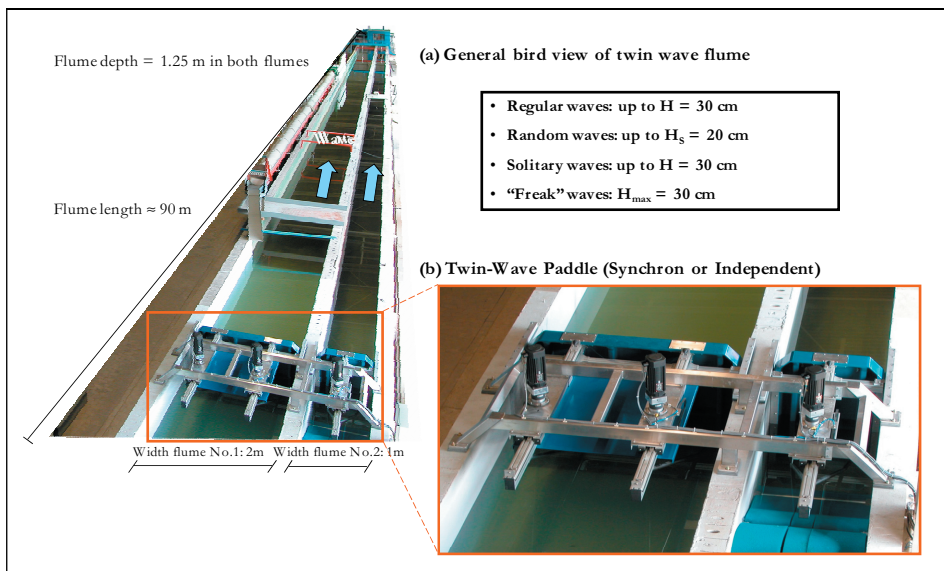


Fig. 5: Twin wave flumes at the Leichtweiß Institute, Technische Universität Braunschweig

2.3 Primary expertise and experience using the Large Wave Flume in brief

A large amount of experience has been gained using the Large Wave Flume during the past 25 years for a wide variety of basic/applied research projects and problems including, in particular:

- (i) *Rubble mound breakwaters*: wave-induced pore pressures within the structure and interactions with external flow, armour stability and structural integrity, pressure on crown walls and overtopping.
- (ii) *Caisson breakwaters*: wave forces and uplift, including breaking-wave impact, pore pressure and soil pressure in the foundation as well as the dynamic response of the structure.

- (iii) *Sea dikes and revetments*: breaking-wave impacts, wave runup and overtopping, stability of revetments, failure caused by overtopping and breaching of sea dikes.
- (iv) *Innovative sea walls and breakwaters*: hydraulic performance, wave loading and stability of high-mound composite breakwaters and sea walls, perforated JARLAN caisson-breakwaters (mono- and multi-chamber systems).
- (v) *Offshore structures*: breaking and non-breaking wave loads on vertical and inclined cylindrical structures, including the dynamic response of pipes on a movable sea bed and seabed scour around pile structures
- (vi) *Beach and dune stability*: profile development during storm surges, including the measurement of suspended load; effect of beach replenishment schemes and low-cost geotextile structures for dune protection.
- (vii) *Submerged wave absorbers for coastal protection*: reflection and wave-damping performance of single and multi-layer submerged permeable walls, effect on beach profile development during storm surge conditions.
- (viii) *Geotextile sand containers (GSC)*: hydraulic stability of GSC used for dune reinforcement, seawalls and seabed scour protection of pile support structures for offshore wind turbines.

A number of such projects are illustrated in Fig. 6.

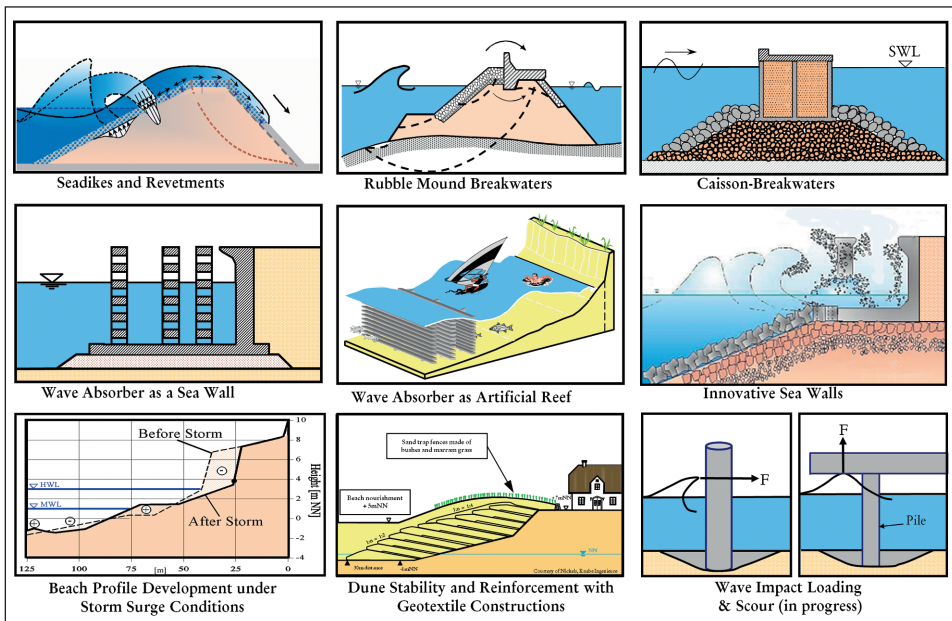


Fig. 6: Selected examples of research projects performed in the GWK

Most of these projects were directed towards a detailed study of the processes involved in wave-structure interaction, wave-seabed interaction and structure-foundation interaction under extreme and/or cyclic loads. As illustrated in Fig. 7 for the example of a vertical monolithic structure subject to wave loading, the primary objective is generally to improve our understanding of the processes that govern the interaction of sea waves with the seabed and the structure as well as the interaction between the structure and its foundation soil. Based on this improved understanding, models (indicated by a transfer function TF in Fig. 7) are then developed to describe these processes and interactions, including an assessment of the associated uncertainties (e.g. coefficient of variation, CoV). The substantial reduction of scale effects and the significant improvement in knowledge achieved so far explain why facilities such as the GWK play a central role in the basic research strategy, as depicted in Fig. 3.

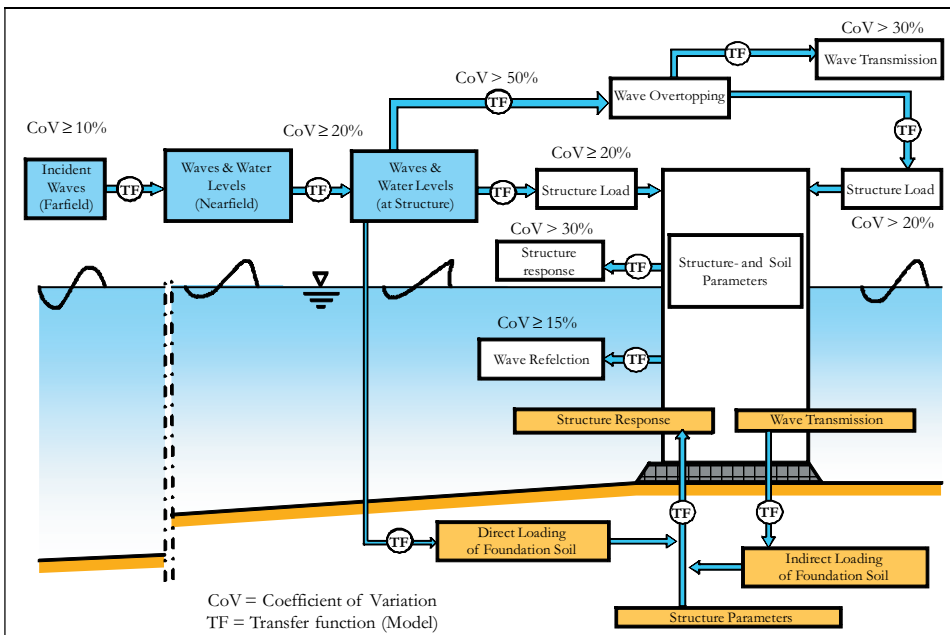


Fig. 7: Processes involved in wave-structure-foundation interactions

In Section 3 that follows, an outline is given of the selected sample projects already listed in the Introduction. These projects extend over several research areas in which the author is involved. As the main purpose of the following is to illustrate the capabilities of large experimental facilities such as the GWK, only a brief description of each project is given. Nevertheless, more detailed references are provided in the last section of the paper and interested prospective readers are invited to contact the author (h.oumeraci@tu-braunschweig.de) for a pdf copy of those references which cannot be easily accessed.

3. Outline of selected research projects performed in the Large Wave Flume (G W K)

3.1 Wave loading and the response of a PBA revetment

Polyurethane bonded aggregate (PBA) revetments are highly porous elastomeric structures made of mineral aggregates (e.g. crushed stone) which are durably and elastically bonded by polyurethane (PU). Despite their numerous advantages compared with conventional revetments and the large experience available from more than 25 pilot projects, physically-based design formulae to predict their hydraulic performance and response to wave loading were still lacking up to 2009. Due to the anticipated scale effects outlined in Fig. 2, particularly those associated with breaking-wave impact loading and foundation response behaviour, large-scale model tests were performed in 2009 in the Large Wave Flume (GWK). These tests were aimed at (i) improving our understanding of the physical processes involved in the interaction of the PBA revetment with waves and the underlying sand core, (ii) developing prediction formulae for hydraulic performance, including wave reflection, wave runup and wave rundown, (iii) developing prediction formulae for the wave loads on and beneath the revetment as well as in the subsoil for a wide range of wave conditions, including both impact and non-impact loads, (iv) developing formulae for the prediction of the response of the revetment (bending) and its foundation (wave-induced pore pressure), (v) reproducing and analysing possible failure mechanisms such as those due to transient soil liquefaction beneath the revetment.

The obtained results and formulae are published in OUMERACI et al. (2010a; 2010b) and OUMERACI et al. (2011). A brief description of the experimental setup and the deployed measuring/observation techniques of one of the key results is given below. This illustrates the capability of such large-scale wave facilities to solve highly complex problems of this type. The selected key result relates to the response of the sand core beneath the revetment (pore pressures), including an analysis of the failure experienced by a tested under-designed revetment alternative.

Further details on how to prepare such complex model tests and how to analyse them within a short period of time to obtain the afore-mentioned formulae/diagrams are given in the research reports by OUMERACI et al. (2009a) and OUMERACI et al. (2009b), respectively, which can be obtained from the author on request.

This example represents one of the several applied research projects performed in close collaboration with industry. Typically, the time taken to implement such results in engineering practice is relatively short. In this case, the time between publishing the final research report (OUMERACI et al. 2010a) and the incorporation of the key results in a design manual for polyurethane bonded aggregate revetments in the Netherlands (ARCADIS, 2010) was only a few months. Further similar Guidelines in Germany and France then followed. A brief outlook is finally provided concerning planned future research directed towards an improved understanding of the processes involved in wave-structure-foundation interaction and numerical modelling.

(a) Experimental setup and testing programme

Three Model Alternatives A, B and C with the same slope 1 : 3 and the same thickness ($\tau_R = 0.15$ m) but with different thicknesses of the gravel sublayer ($\tau_R = 0.0$ m; 0.10 m and 0.20 m) were tested in the GWK (Fig. 8).

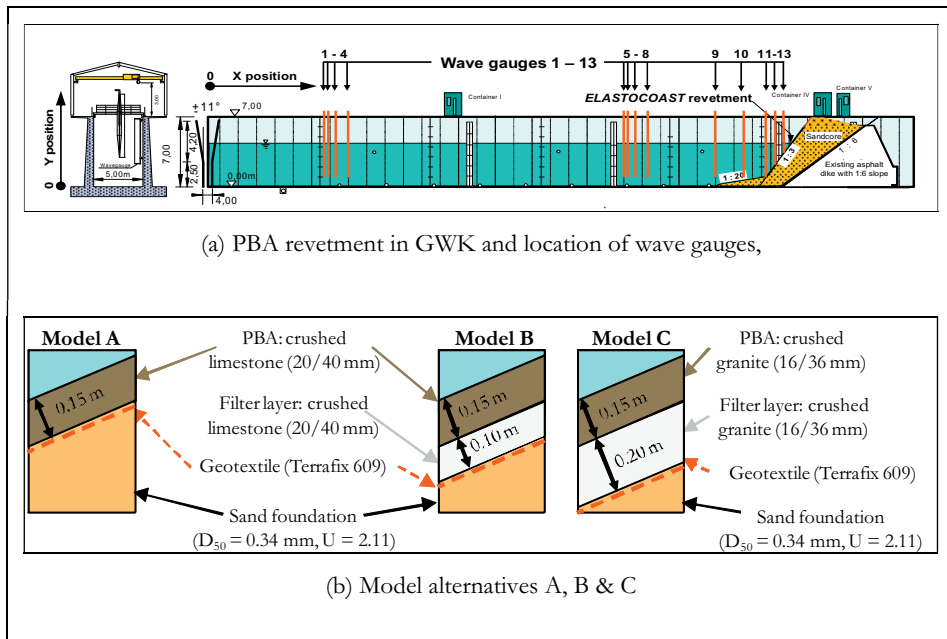


Fig. 8: Experimental setup for PBA revetments in the GWK

The embankment was constructed of sand with a grain size of $D_{50} = 0.34$ mm, $D_{10} = 0.18$ mm and $U = D_{60}/D_{10} = 2.11$. The foreshore of the PBA revetment (slope of 1 : 3) is a sand bed with a slope of 1 : 20. The toe of the revetment is located 1.0 m above the flume bottom while the crest of the revetment extends up to 6.70 m just below the top edge of the flume, which is located at height of 7.00 m (Fig. 8).

In a first phase, the model setup consisted of two alternative revetments. The two model alternatives A and B were constructed together side by side, each covering half of the wave flume width (2 x 2.5 m), and were tested simultaneously under the same wave conditions (Fig. 9).

Both model alternatives have a PBA layer of the same thickness ($d = 0.15$ m) made of the same crushed limestone (20/40 mm) bonded together by the same polyurethane. The only difference between the two models consists in the layer beneath the PBA (Fig. 8a; b). For Model Alternative A the PBA lies directly on a geotextile filter, while for Model Alternative B the PBA lies on a gravel sublayer with a thickness of 0.10 m. The same crushed limestone material (20/40 mm) was used in each case. The gravel sublayer is inserted between the PBA layer and the geotextile filter lying on the sand slope (Fig. 8b). The two alternatives are separated by a thin wall made of water-resistant plywood (OUMERACI et al., 2009a; 2009b).

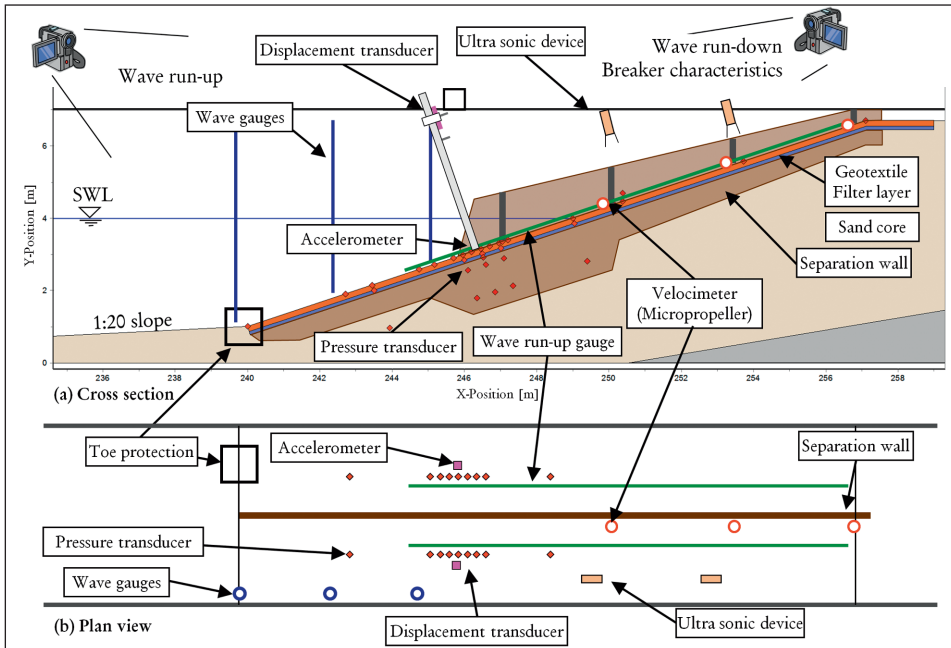


Fig. 9: Measuring and observation devices along and beneath the revetment

Following damage of Model Alternative A, the damaged revetment was completely removed and replaced by a third Model Alternative C (Fig. 8c). This alternative is essentially similar to Model Alternatives A and B. In this case, however, the PBA layer consists of crushed granite stones (16/36 mm) while the thickness of the sublayer made of the same stones is now 0.20 m, which is twice as large as in Model Alternative B.

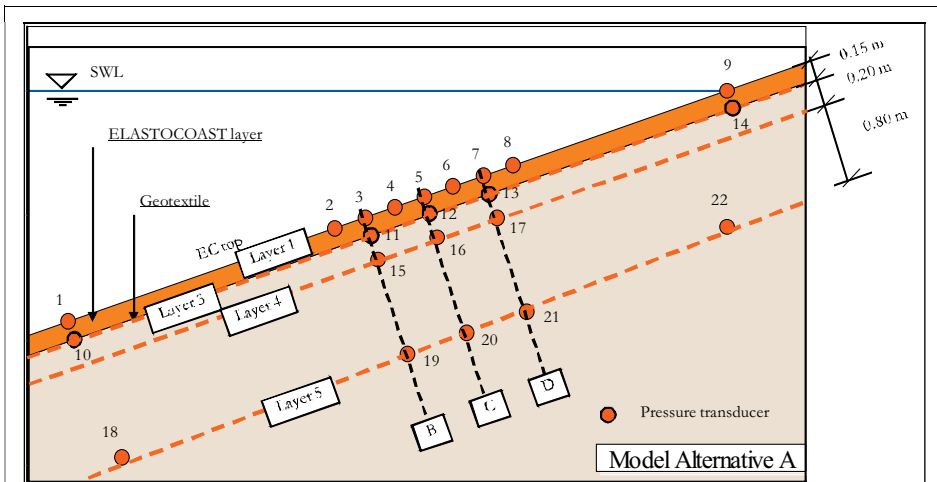
A total of 86 measuring devices synchronized by two digital video cameras were used to record the waves in the far and near field, wave runup and rundown, runup layer thickness and velocity, pressures on and just beneath the revetment, pore pressure in the subsoil as well as motions of the revetment normal to the slope. The types and optimum locations of these devices were determined by a preparatory study, applying available empirical formulae and numerical modelling (OUMERACI et al., 2009a).

More than 35 tests with regular waves ($H = 0.2-1.3$ m, $T = 3-8$ s, $h = 3.4-4.2$ m, 100 waves/test) and more than 40 tests with irregular waves ($H_s = 0.2-1.1$ m, $T_p = 3-8$ s, $h = 3.4-4.2$ m, 1000 waves/test) were performed, including a few tests with solitary waves and “wave focussing”. As the major aim of the study was to derive empirical formulae/diagrams for design purposes, attention was focussed on an analysis of the experiments involving wave spectra.

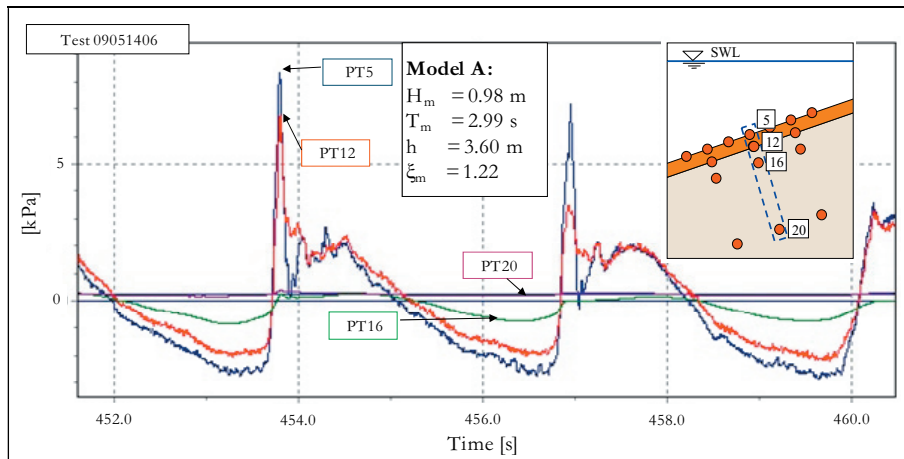
(b) Wave-induced pore pressure in the sand core beneath the revetment

In addition to the wave pressure on and just beneath the revetment measured by pressure transducers (PT) in layers 1 and 2, respectively, pore pressure induced in the sand core beneath the revetment were also measured in layers 3, 4 and 5 and at different locations B, C and D, as shown by way of example for revetment Model Alternative A in Fig. 10.

The analysis of wave-induced pore pressure in the sand core beneath the revetment, including both transient and residual pore pressure, represents an important part of the study. As the former was found to be more critical regarding the stability of the sand core beneath the revetment, formulae were developed for transient pore pressure only. These formulae show that the pore pressure is almost completely damped at a depth of about 80 cm in the sand core beneath the revetment. For more detailed and further results refer to OUMERACI et al. (2009b; 2011).



(a) Pressure transducers in layers 1-5 and at locations B, C and D for Model Alternative A (without a gravel filter)



(b) Pressure histories recorded by way of example for Model A

Fig. 10: Pore pressure induced beneath the revetment (for Model A in Fig. 8b)

(c) Failure of under-designed revetments: brief description and analysis

Brief description of failure: as shown in Figs. 11 and 12, the failure of revetment model A (Fig. 8) occurred under regular wave attack with $H = 1.3$ m and $T = 5$ s for a water depth of $h = 3.90$ m. No failure occurred in Model B (Fig. 8), which was tested simultaneously under exactly the same wave conditions.. In a previous test with the same water depth ($h = 3.90$ m), the same wave height ($H = 1.3$ m), but with a shorter wave period ($T = 4$ s), no apparent damage occurred in Models A and B.

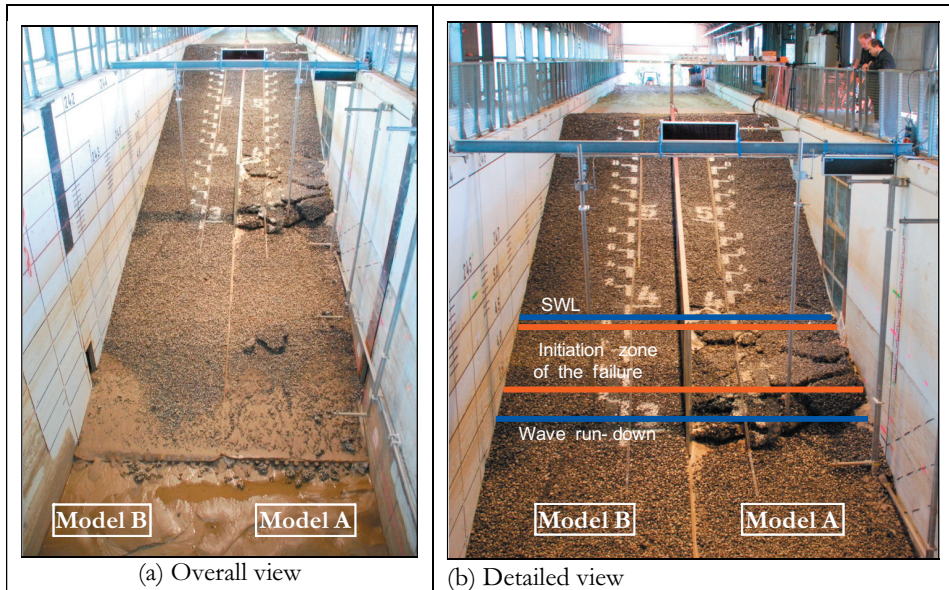


Fig. 11: Extent of damage of revetment Model A (induced by regular waves)

The exact time at which the collapse of Model A occurred is identified by the displacement meter recordings given in Fig. 12, which shows a comparison of the recorded displacements for Model A and Model B. It is seen that the collapse of Model A occurred after $t = 450$ s ($t = 7:30$ min), i.e. between the 74th and the 75th wave of the respective test.

The onset of failure began just after $t = 430$ s ($t = 7:10$ min), i.e. just after the 70th wave, when a residual upward displacement rapidly developed during each cycle until collapse occurred. The uplift of the revetment during each wave cycle causes a gap to develop beneath the revetment, which allows sediment to move more freely. As a result, the residual upward displacement increases progressively until collapse occurs. The maximum residual upward displacement (15 mm) was recorded by the displacement meter during run-down of the 75th wave, which caused the revetment to collapse. As observed visually during the tests, the collapse occurred within a very short time interval (a few seconds) without any visually perceptible precursors. Following the significant upward motion of the revetment and the resulting gaps beneath the revetment, a considerable amount of sand was washed out by the receding waves on the slope (downrush flow). As a result, significant settlement of the revetment and

subsequent failure occurred. As shown in Fig. 11a, the washed-out sand was deposited at the toe of the revetment. Fig. 11a together with Fig. 11b show that the occurrence of collapse was spatially concentrated just below still water level. In comparison, no build up of residual displacement (Fig. 12) and no damage (Fig. 11) occurred in Model B, which was subject to the same incident waves as Model A.

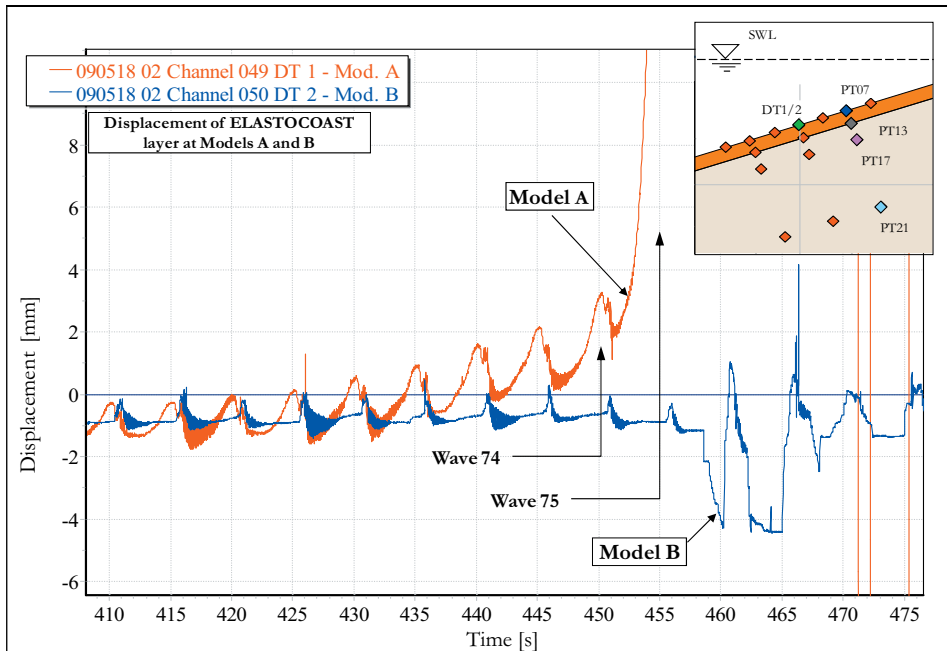


Fig. 12: Displacement signals for Models A and B at the time of failure (Model A)

The primary difference between Model A which failed and Model B which did not fail under the same wave conditions is the 10 cm thick gravel sublayer (Fig. 8b), which provides additional weight and stiffness to Model B. This results in greater resistance against failure (e.g. reduction of shear resistance and liquefaction) of the sand core beneath the revetment, which is subject to different pore pressures in each of the two models.

Although the wave pressure on and beneath the revetment is almost identical in Models A and B, the uplift pressure in Model A is slightly higher than in Model B (OUMERACI et al., 2009a; 2009b). However, the response of the sand core beneath the revetment is different in the two models. The “negative” pore pressure amplitudes measured 20 cm beneath the upper boundary of the sand core by pressure transducer PT17 in Model A and by PT43 in Model B differ significantly, while the “positive” pore pressure amplitudes are in the same range for both models. In fact the “negative” pore pressure amplitudes in Model A are almost twice as high as in Model B. The extremely higher “negative” pressure gradient beneath Model A induced a significantly stronger upward water flow in the sand core beneath the revetment compared to Model B. It should be noted that this is valid for the pore pressure signals re-

corded long before the failure of Model A occurred, and that about 10 waves before collapse at $t = 455$ s, the pore pressure amplitudes remained almost constant over time. This is surprisingly not the case for the last 10 waves prior to failure. As shown in Fig. 13, the “negative” pore pressure amplitudes recorded by PT17 in Model A progressively increase from -2.4 kPa at $t = 410$ s to -3.2 kPa at $t = 445$ s, i.e. just before incipience of failure, while the “positive” pore pressure amplitudes remain almost constant over time. At the onset of failure (74th wave at $t = 450$ s), the pore pressure decreased to -5.6 kPa and dropped to -11.4 kPa as the revetment collapsed (75th wave at $t = 455$ s).

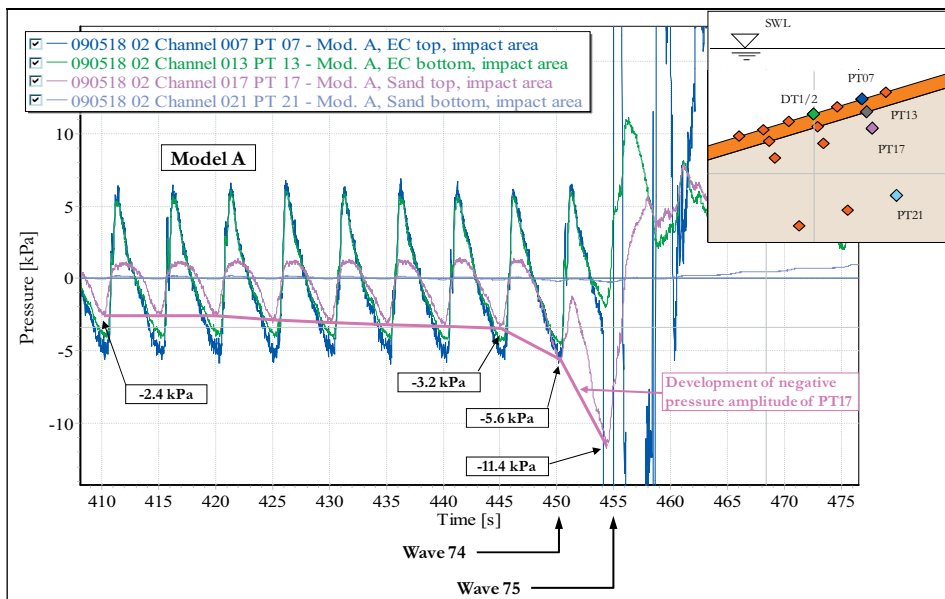


Fig. 13: Pore pressure development in the sand core beneath the revetment of model A just before collapse

As shown by the simultaneously measured displacement of the revetment, the progressive increase in the “negative” pore pressure amplitude is accompanied by a simultaneously progressive increase of the upward displacement of the revetment up to the point of failure.

These results indicate that the failure of Model A is most probably caused by transient liquefaction of the sand core beneath the revetment. To confirm this result, a comparative stability analysis of Models A and B for the same tests, during which failure of Model A occurred, is outlined below. Further details of the analysis are given in the final report (OUMERACI et al., 2010a), which may be obtained from the author as a pdf file on request (h.oumeraci@tu-braunschweig.de).

Brief analysis of failure: Although residual pore pressure in coarse sand is relatively rare or not significant under wave action alone, both the residual pore pressure u_r and the transient pore pressure u_t should be taken into consideration in the loading term $((u_0 - u_r) + u_t)$ in a stability analysis relating to soil liquefaction at each depth z' in the sand core beneath the revetment. This is carried out as illustrated schematically in Fig. 14. The resistance term (initial

effective stress σ'_{v0} is provided by the submerged weight of the soil (σ'_{v0s}) and that of the revetment (σ'_{v0r}) at the corresponding depth z' beneath the surface of the sand core. If the loading term $((u_0 - u_r) + u_r)$ at a certain location z' in the sand core attains the effective stress σ'_{v0} , soil liquefaction will occur at that location (Fig. 14).

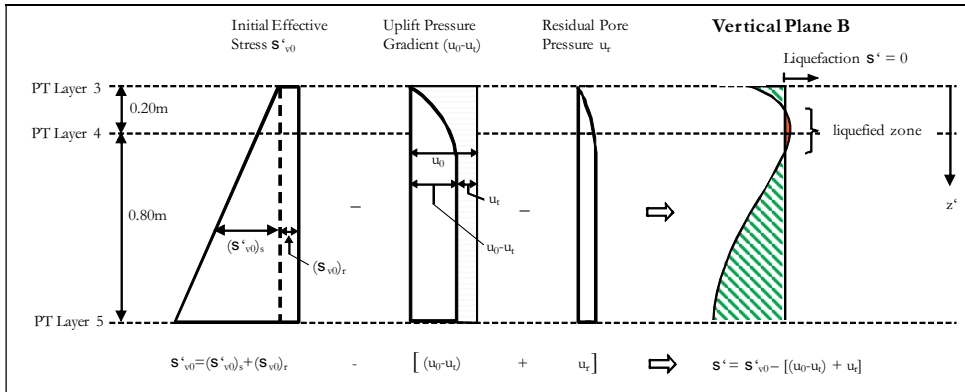


Fig. 14: Stability analysis relating to soil liquefaction beneath the revetment (definition sketch)

Following this procedure, the results of the stability analysis for Model A (Test 09051802) are given in Fig. 15a. This indicates that transient liquefaction indeed occurred around PT Layer 4 for $H = 1.4$ m, $T = 5$ s and $h = 3.9$ m. A comparison with the stability analysis of Model B for the same regular wave test (Fig. 15b) illustrates why Model B did not fail. In fact, the effective stress σ' around PT Layer 4 fell to a very low level ($\sigma' = 0.43$ kN/m²) close to the failure level.

In overall terms, the results have substantially contributed to improving our understanding of the physical processes involved in wave-structure-foundation interaction. Nevertheless, further research is still required to further improve our understanding of how to predict the stepwise failure of the subsoil and the steps necessary to develop a coupled CFD-CSD model capable of describing (i) the wave field in front of the porous slope structure, the detailed external flow on, in and just beneath the revetment as well as the coupled internal flow in the underlying filter layer and sand core and (ii) the bending deformations and stresses in the revetment as well as the pore pressures and effective stresses in the sand core beneath the revetment.

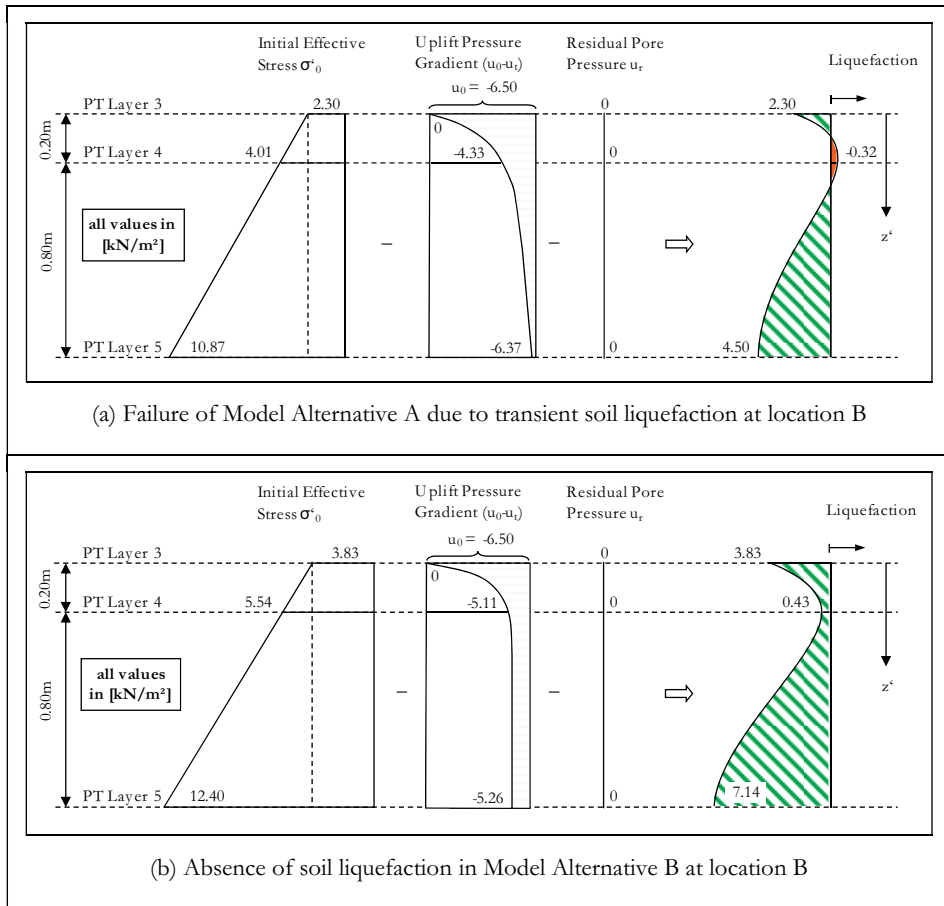


Fig. 15: Comparative stability analysis for Models A and B under the same wave conditions (test 09051802 with $H = 1.4$ m, $T = 5$ s, $h = 3.9$ m)

3.2 Wave loading and the response of a caisson breakwater foundation

A further example to illustrate the necessity and capability of large-scale wave facilities such as the GWK is the wave loading and response of the foundations of gravity structures such as caisson breakwaters. In this case, scale effects would be expected particularly with regard to breaking-wave impact loads as well as pore pressure generation and dissipation in the soil beneath the gravity structure (OUMERACI, 2004; OUMERACI et al., 2001b). Large-scale tests are therefore generally required to avoid/reduce these scale effects. In contrast to the slope revetment described above in Section 3.1, transient pore pressure is not likely to affect foundation stability in this case. For complete or even partial liquefaction to occur during storm surges, very unfavourable wave-loading and drainage conditions would be required in order to create residual pore pressure in the soil beneath the structure foundation, i.e. condi-

tions that are rarely encountered in the case of normal marine structures. This is confirmed by the results of the analyses of more than 20 failures of vertical breakwaters (OUMERACI, 1994b). The conclusions of the latter study stress the relative importance of the contribution of geotechnical failure modes, but exclude any occurrence of complete residual liquefaction beneath caisson breakwaters. However, under the combined action of both wave and caisson motions, a considerable build-up of pore pressure beneath the caisson may occur, induced by residual soil deformations (OUMERACI, 1994b; OUMERACI et al., 2001b). To confirm these findings, large-scale model tests on a caisson breakwater were performed in the GWK within the framework of the European Project LIMAS (Liquefaction Around Marine Structures).

(a) Experimental setup and testing programme

The model of the caisson breakwater was located about 240 m from the wave generator. The cross-section of the breakwater model, including the positions of the transducers installed on the caisson and its foundation are shown in Fig. 16. The sand beneath the caisson was selected to be as fine as practicably feasible with a mean grain size of $D_{50} = 0.21$ mm, $D_{10} = 0.13$ mm and a non-uniformity coefficient $U = 1.69$. The initial density index I_D was estimated to have an average value of $I_D = 0.21$. Despite the flushing process, the achieved saturation level was still below $S_r = 1$.

The caisson was placed on a 20 cm thick rubble layer. In order to simulate unfavourable drainage conditions of the soil comparable to a loose sand bed with thin clay or silt layers, the sand beneath the breakwater was enclosed in almost impermeable sheets (Fig. 16). The deployed measuring devices were selected to provide simultaneous records of the incident and reflected waves, the wave loading on the structure, the caisson motion, the induced pore water pressure and the mean total stress within the soil foundation. In the sand bed beneath the caisson, 26 pressure transducers for measuring pore water pressure and total stresses were installed using a fixed frame (Fig. 16). The pressure transducers in the soil foundation were positioned in such a way that it is possible to distinguish the pore pressures induced directly by wave motion propagating into the soil from those indirectly induced as a result of caisson motion. In order to measure the wave load and the dynamic response of the caisson, a total of 14 measurement devices were installed on the caisson. These consisted of 10 water pressure transducers for determining the wave loads on the caisson, three displacement meters for measuring the dynamic response, and a wave gauge for measuring wave runup and run-down on the caisson face (Fig. 16). An additional wave gauge over the berm and a pressure transducer along the outer edge of the berm provided the input pressure and water surface elevation just before reaching the measurement area. 18 wave gauges were additionally installed along the flume.

The testing programme was devised to obtain both pulsating wave loads and breaking wave impact loads according to the PROVERBS parameter map for defining the type of wave loads, as proposed by OUMERACI et al. (2001b) and OUMERACI (2004). The tests were carried out with regular waves ($H = 0.4$ – 0.9 m, $T = 4.5$ – 6.5 s) and wave spectra ($H_s = 0.4$ – 0.9 m, $T_p = 4.5$ – 8 s). The water depth was held constant at $h = 4.05$ m in the far field and $h = 1.60$ m at the toe of the breakwater berm (Fig. 16).

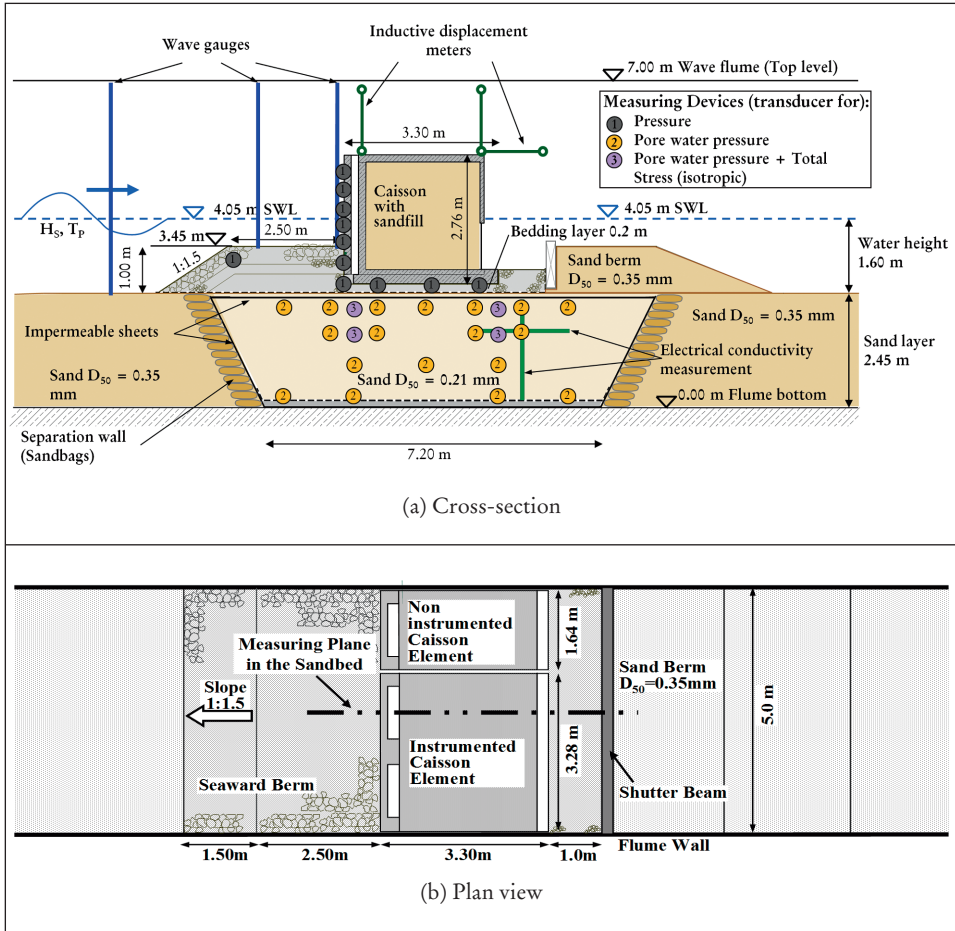


Fig. 16: Experimental setup and location of measuring devices in the caisson breakwater model (KUDELLA and OUMERACI, 2004)

(b) Residual pore pressure and residual soil deformations

Under the testing conditions described above, the transient pore pressures in the seabed beneath the back of the caisson are essentially generated by caisson motions $d_{v,b}(t)$ (hereafter referred to as “caisson mode”). These pore pressures are an order of magnitude higher than those induced directly by the waves in front of the caisson (hereafter referred to as “wave mode”). Consequently, the contribution of the wave mode to residual pore pressure generation is likely to be negligible and the caisson motion $d_{v,b}(t)$ can be considered to exclusively represent the input parameter for the generation of residual pore pressure in the seabed beneath the caisson. On the other hand, it was found that threshold values of the frequency and amplitude of the caisson motions $d_{v,b}(t)$ are required for initiating residual pore pressure generation. Although these were not attained in the case of pulsating wave loads, they were

greatly exceeded in the case of impact loads (KUDELLA and OUMERACI, 2005; KUDELLA et al., 2006). In fact, the latter induce caisson motions with an amplitude and frequency of an order of magnitude greater than those induced by pulsating wave loads. With regard to the generation of residual pore pressure, attention was thus focussed on an analysis of the tests with breaking-wave impact loads. An example of this residual pore pressure generation mechanism is given in Fig. 17, which indicates both transient and residual traces of the vertical caisson motion $d_{v,b}(t)$ and pore pressure response $u(t)$ along the rear face of the caisson (P36).

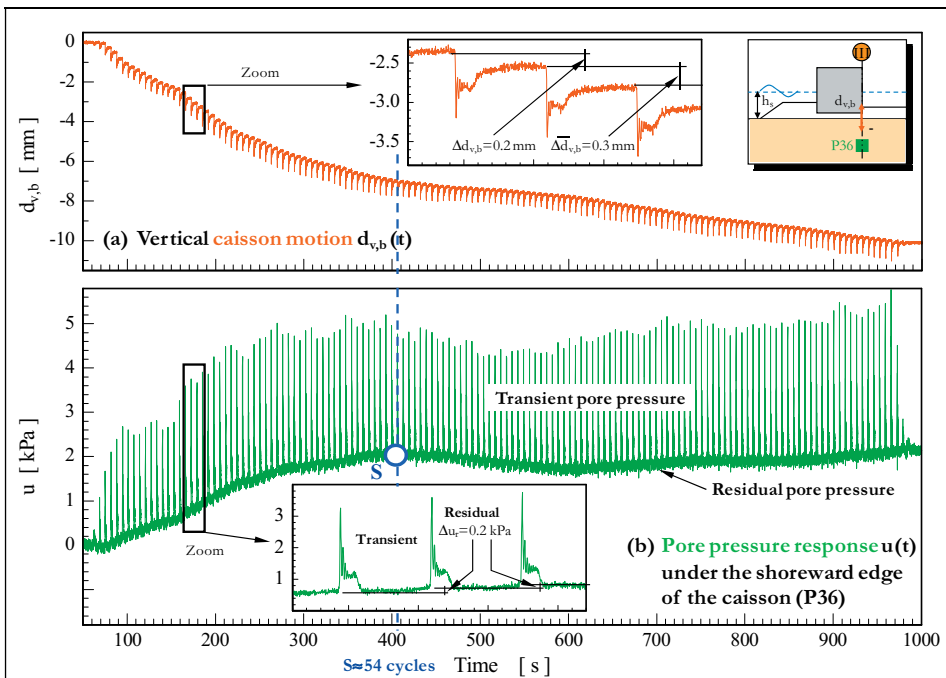


Fig. 17: Transient and residual pore pressure generation induced by caisson motion ($H = 0.6$ m, $T = 6.5$ s, $h_s = 1.6$ m, $h_1 = 0.6$ m) (KUDELLA and OUMERACI, 2005)

This result also shows that there is a close correlation between residual pore pressure and settlement, i.e. soil deformations. Three stages of pore pressure generation/dissipation are observed for the tested conditions: (i) generation dominates dissipation; (ii) there is a quasi-equilibrium between generation and dissipation and (iii) residual pore pressure exclusively dissipates. The latter stage commences right at the end of the tests (no wave action) and is characterized by an exponential decrease of residual pore pressure with time (KUDELLA and OUMERACI, 2004). Moreover, the pulsating wave loads are unable to generate residual pore pressure because the induced caisson motions are too small. The critical downward amplitude of the caisson motion, for which the generation of residual pore pressure starts, is tentatively estimated to be $(d_{v,b})_{crit} = -0.3$ mm (KUDELLA and OUMERACI, 2004; 2005; KUDELLA et al., 2006).

Once this threshold value is exceeded, the rate of increase of residual pore pressure is strongly determined by the density index I_D of the soil. The lower the density I_D , the higher is the rate of increase of residual pore pressure.

The results shown in Fig. 17 suggest that there is a very close correlation between residual pore pressure u_r and residual soil deformations $d_{v,b}$. The stepwise generation of the residual components of the pore pressure and caisson motion ($\Sigma(\Delta(u_r)_i$ and $\Sigma\Delta(d_{v,b})_i$) caused by the transient components $u_t(t)$ and $d_{v,b}(t)$ after exceeding a certain threshold value is indicated in Fig. 17. This has been investigated in more detail by KUDELLA and OUMERACI (2004) for both vertical and horizontal motions and on both the seaward and shoreward faces of the caisson.

In order to illustrate and discuss this correlation, the wave load $M_t(t)$ (M_t = total moment around the caisson heel induced by the horizontal impact force and the uplift force), the associated vertical oscillatory caisson motions $d_{v,b}(t)$ (transient component), the transient pore pressure response $u_t(t)$ as well as the associated residual components $u_r(t)$ and $d_{v,b}(t)$ on the shoreward face of the caisson are plotted in Fig. 18 for 692 wave load cycles corresponding to a test duration of about 1.25 hours.

Although the moment peaks $M_{t,max}$ over the entire test duration do not vary significantly around the mean value $M_{t,max} = 210 \text{ kNm/m}$, the transient components of the caisson motions $d_{v,b}(t)$ and pore pressure $u_t(t)$ start to increase after 128 load cycles. This results in the “Inflexion Point” I of the response curves of the residual components $d_{v,b}(t)$ and $u_r(t)$, i.e. after Point I, the generation of residual pore pressure becomes more dominant and both $d_{v,b}$ and u_r increase at a higher rate up to a “Saturation Point” S where the generation and dissipation of residual pore pressure are in balance. After Point S, where the residual pore pressure ratio u_r/σ'_{v0} was determined to be about 0.5 (no liquefaction), the residual pore pressure decreases while the residual soil deformation (settlement) still increases. A quantitative analysis of the relative contributions of the generation and dissipation process has been conducted in KUDELLA and OUMERACI (2004). This analysis shows that the generation gradient of pore pressure starts to decrease after point S due to increasing compaction of the subsoil. Because the dissipation gradient remains constant, this leads to a decrease in the $u_r(t)$ curve beyond the “Saturation Point” S.

Even under unfavourable drainage and soil conditions of the seabed beneath a caisson breakwater (thin clay or silt layers in a relatively loose sand bed) as well as under very severe conditions of wave loading of the structure (breaking wave impacts), only one fourth of the critical residual pore pressure ratio ($u_r/\sigma'_{v0} = 1.0$) for total residual liquefaction was attained. Nevertheless, the analysis of the initial results has thrown light on the processes that may lead to partial and total liquefaction of a sand bed beneath a caisson breakwater under unfavourable conditions. Among others, it was found that: (i) the generation of both transient and residual pore pressure is essentially due to caisson motions, and that the latter should be of sufficiently high frequency and magnitude to generate residual pore pressure; (ii) such large and high frequency caisson motions can only be induced by severe breaking-wave impacts and (iii) a very close correlation exists between residual pore pressure and residual soil deformations beneath the breakwater. This can be quantified definitely by a more detailed analysis of the balance between pore pressure generation and dissipation processes (KUDELLA et al., 2006).

As critical residual soil deformations which may lead to the collapse of a breakwater can also occur at low values of the residual pore pressure ratio u_r/σ'_{v0} , a future analysis of the results, combined with numerical modelling, will focus on a closer examination of the balance between pore pressure generation and dissipation in order to develop design guidelines based on allowable soil deformations (OUMERACI, 1994b).

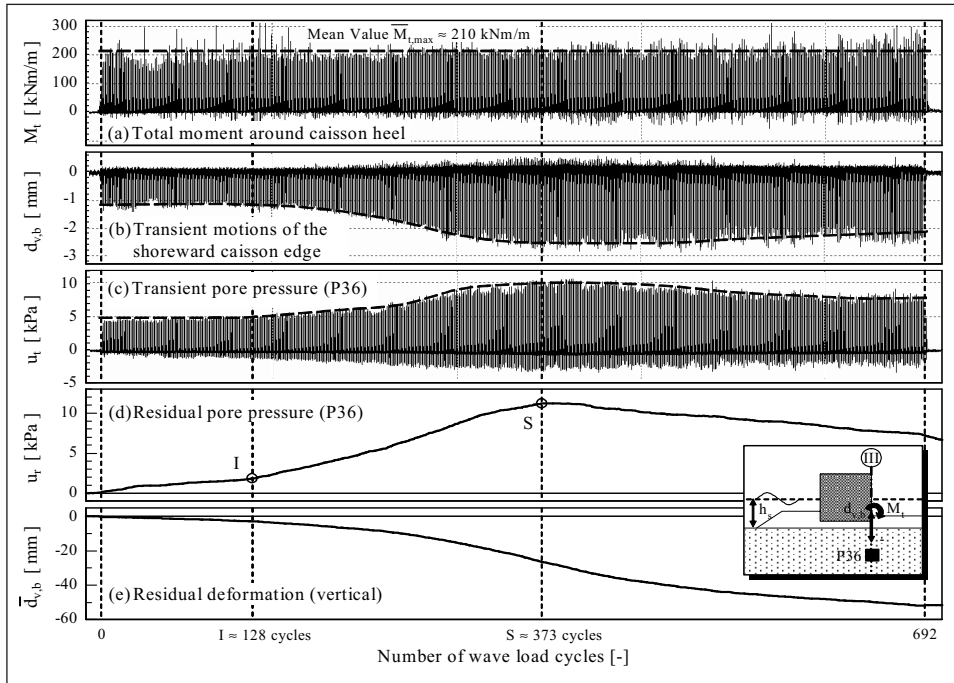


Fig. 18: Wave load, pore pressure response and soil deformation ($H = 0.9$ m, $T = 6.5$ s, $h_s = 1.6$ m, $h_1 = 0.6$ m) (KUDELLA and OUMERACI, 2004; 2005)

3.3 Hydraulic performance of wave damping structures

Increasing interest in the practical implementation of sustainability principles in coastal engineering (OUMERACI, 2000) will require more effort on the part of engineers to develop innovative structures with improved wave-damping performance, lower environmental impact, and lower capital and maintenance costs for the proper sheltering of harbours and other marine facilities. This also includes, of course, the effective protection of coasts threatened by storm surges.

To illustrate the process of developing and testing non-conventional structures and the role of large-scale testing facilities in this process, selected research studies performed in recent years by the Leichtweiß Institute (LWI) in the GWK (see Fig. 19) are briefly summarized below. These studies were aimed at achieving (i) a better understanding of the hydraulic functioning and limitations of existing concepts, (ii) a clear identification of their drawbacks with respect to commonly accepted and newly emerging performance characteristics/requirements and (iii) a better control of the physical processes and structure parameters which contribute to the improvement of hydraulic performance and a reduction of wave loading (OUMERACI, 2010a).

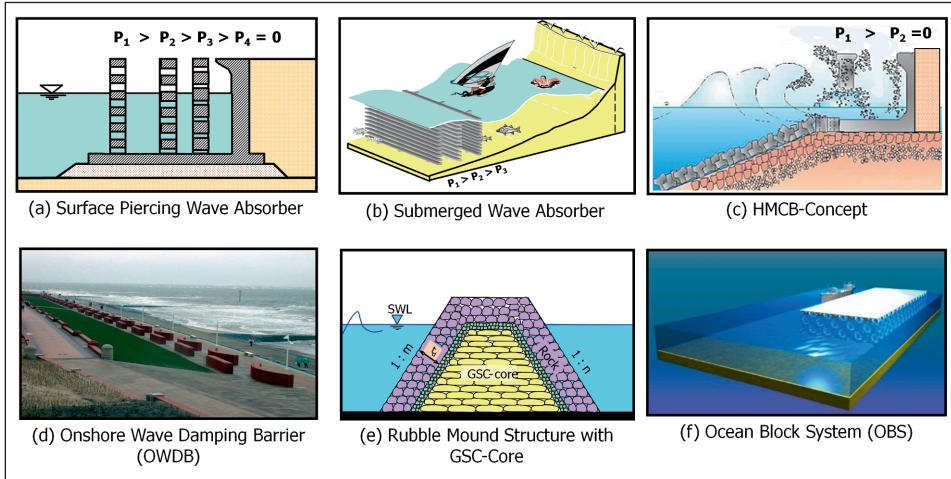


Fig. 19: Selected innovative wave-damping structures tested by the LWI (first four tested in the GWK)

(a) Surface-Piercing Wave Absorber (Multi-Chamber Caisson)

One of the most useful concepts to cope with the high reflection caused by vertical face breakwaters and sea walls is the perforated JARLAN-type breakwater, which was introduced in Canada in 1960 (BERGMANN, 2001). This consists of a single wave-energy dissipation chamber bounded on the seaward side by a perforated front wall (porosity $\varepsilon \approx 20\%$) and shoreward by an impermeable back wall (One Chamber System). The incident wave energy is partly reflected at the front wall and partly transmitted through the perforations into the wave chamber, where a certain amount of the incident wave energy is reflected by the back wall. The major part of the incident wave energy, however, is dissipated due to resonance phenomena, vortices and friction losses. Although the relative significance of the reflected and dissipated components of the total incident wave energy, and hence the hydraulic performance of the system, depend on the porosity of the front wall, it is essentially governed by the ratio of the chamber width B to the wave length L of the incident waves (B/L).

Although the JARLAN-type breakwater concept has been applied more or less successfully worldwide, it has a basic drawback (see Fig. 6), which requires further development of the concept. For this purpose, it was necessary to first investigate the key processes which contribute to wave damping by friction (local losses and vortices) and by destructive interference of the incident and reflected waves over the full range of B/L ratios (i.e. over the full range of incident wave periods). The results of the large-scale tests in the GWK illustrate well how a traditional JARLAN-type caisson functions (OUMERACI, 2010a).

As shown by the upper curve in Fig. 20, the traditional JARLAN-type caisson (OCS) has, a much lower reflection coefficient (and thus a much larger energy dissipation) than a vertical impermeable wall at its optimum working point ($B/L \approx 0.2$). However, the response is very selective with respect to incident wave periods, i.e. it performs satisfactorily only within a very narrow band of B/L ratios.

In order to overcome this drawback, a new Multi-Chamber System (MCS) was developed and tested in the Large Wave Flume (Fig. 19a). As shown by the lower curve in Fig. 20,

the new MCS concept not only provides a lower reflection coefficient, but this reflection coefficient remains at its lowest possible level over the full range of practical B/L ratios (i.e. for $B/L > 0.25$, where B is defined as the overall width of the Multi-Chamber System). In addition to a substantial improvement in hydraulic performance achieved by the new multi-chamber concept, the new concept also has the advantage of greatly reducing the resulting horizontal wave forces F_{total}^+ (obtained by superposition of the forces acting simultaneously on each wall). Because wave forces are directly related to water surface elevation and thus to wave reflection (BERGMANN and OUMERACI, 2008), the total force F_{total}^+ (related to the force $F_{0\%}^+$ on a single impermeable vertical wall with zero-porosity) exhibits very similar behaviour to the reflection coefficient with respect to the B/L ratio. Further results can be found in BERGMANN (2001), BERGMANN and OUMERACI (2000; 2001; 2002; 2008) and OUMERACI (2004).

This first sample study illustrates how a detailed insight into the physical processes responsible for the hydraulic functioning of an existing system may lead to a clear identification of the drawbacks of this system by indicating how to overcome these drawbacks and how to achieve substantial improvements through the introduction of new structural members. Given its potential to substantially reduce and better control wave reflection (less risk to navigation and less seabed scour), wave loads, wave runup and overtopping, spray generation, etc., the new Multi-Chamber System represents an ideal alternative as a breakwater, jetty and quay wall as well as a sea wall for the protection of reclaimed sea fronts and artificial islands. Due to the flexibility of caisson structure design regarding shape and size, sea walls may be adapted to incorporate promenades and other facilities for recreational activities, etc. (OUMERACI, 2004).

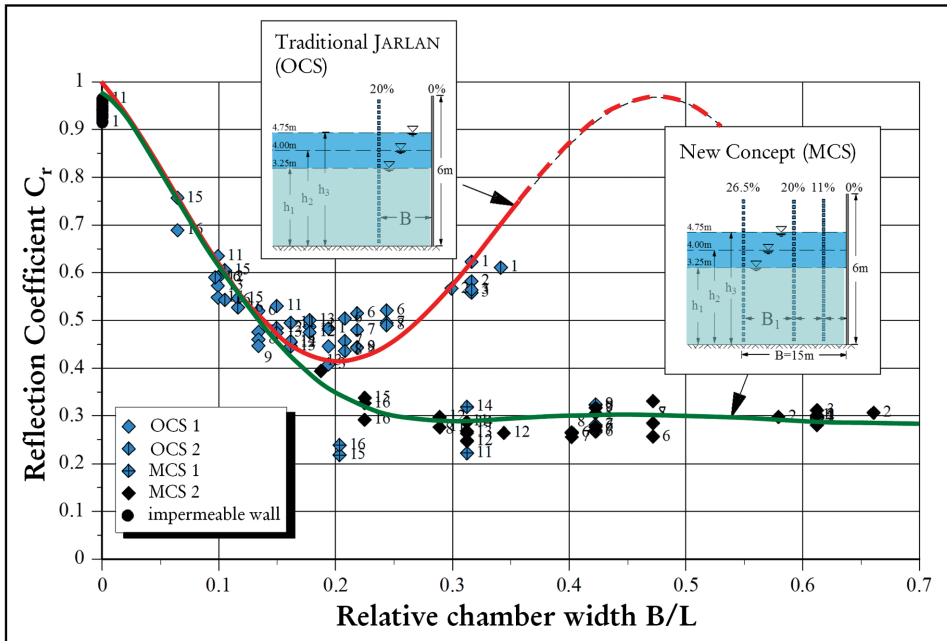


Fig. 20: Reflection coefficient vs. relative chamber width for a traditional JARLAN-Type caisson and for the new Multi-Chamber System (OUMERACI, 2010a)

(b) Submerged Wave Absorber for Shore Protection

An interesting cost-effective and soft alternative to conventional sea walls for coastal protection against erosion are artificial reefs which have the advantage that: (i) they attenuate waves before they reach the shoreline; (ii) they are not visible to viewers on the beach and therefore do not affect the marine landscape; (iii) they serve to reduce the morphological impact on the foreshore (erosion) and on the neighbouring coast (down-coast erosion) and (iv) they ensure water exchange between the open sea and the sheltered area (KOETHER, 2002).

However, existing artificial reef concepts also have serious drawbacks: the wave-damping performance is limited; the overall hydraulic performance is difficult to control due to the limitations associated with a variation of structural parameters, etc. A reef concept consisting of submerged permeable screens with predefined porosity (progressively decreasing in the wave direction) and spacing was thus tested experimentally in the Large Wave Flume (GWK). As schematically shown in Fig. 19b for a three-filter system, this reef concept is particularly suitable for the protection of coastal areas frequently used for recreational activities.

Before commencing with the systematic study of the hydraulic performance of this new reef concept, it was important to first demonstrate its efficiency regarding protection against beach erosion. For this purpose, a submerged two-filter system with porosities $\varepsilon = 11\%$, (front screen) and $\varepsilon = 5\%$ (back screen), spacing $B = 10.3$ m and height $d_b = 4$ m was installed in front of a beach profile. The same beach profile was previously tested in the Large Wave Flume (GWK) (NEWE, 2002) without any protection under the same storm surge conditions (storm surge water level $h = 5.0$ m, TMA wave spectrum with a significant wave height $H_s = 1.20$ m and a peak period $T_p = 6.6$ s, test duration $t = 10$ hours). A comparison of the results relating to the development of the beach profile with and without the reef structure is shown in Fig. 21. These results clearly demonstrate the efficiency of the new reef concept as a soft protection alternative. It is found in fact that beach erosion, seaward transport and sand bar formation occurs in both cases (i.e. with and without protection). However, the transport rate in the case of the unprotected beach is about twice as large as the transport rate for the protected beach. In addition, the reef causes seaward transport to occur only within a limited narrow zone. This means that the resulting sand bar with a reef does not extend as far seawards as in the case of an unprotected beach. Moreover, the eroded volume above the storm water level ($h = 5.0$ m) for the protected beach is only half as much as the eroded volume for the beach without any protection. As a result, the recession of the shoreline (at still water level) of the protected beach is only half as much as that of the unprotected beach (Fig. 21) (see KOETHER, 2002).

Regarding the hydraulic performance of submerged wave absorbers, the results with a two-screen and three-screen wave-absorber systems clearly indicate that for a given submergence depth (R_c/H_s), the relative spacing between the screens B/L is the most decisive parameter for describing the hydraulic performance of a wave-absorber system (OUMERACI and KOETHER, 2009). For instance, the contribution of the seaward screen to the total wave-damping of a two-screen system varies between 30 % for $B/L \approx 0.5$ and 85 % for $B/L \approx 0.3$. The maximum wave-damping performance of the system also occurs for $B/L = 0.3$, while the minimum value is for $B/L = 0.5$.

From the comparative analysis of the hydraulic performance shown in Fig. 22 for a submerged single screen with different porosities ($\varepsilon = 0\%$, 5% and 11%) and submerged two- or three-screen systems, it is seen that: (i) using a filter system instead of a single screen

substantially increases the amount of dissipated energy; (ii) unlike a single screen, a filter system can substantially reduce and control both wave reflection and wave transmission; (iii) using an optimised three-filter system, more than 80 % of the incident wave energy can be dissipated; (iv) the relative submergence depth R_c/H_i is an important parameter for describing the wave-damping performance of both single screens and filter systems and (v) for the range of practical submergence depths ($R_c/H_i \approx -1$), the greatest improvement in wave-damping performance is achieved using a two-filter system instead of a single filter system. A further increase in the number of filters would lead to a comparatively lower improvement in wave-damping performance.

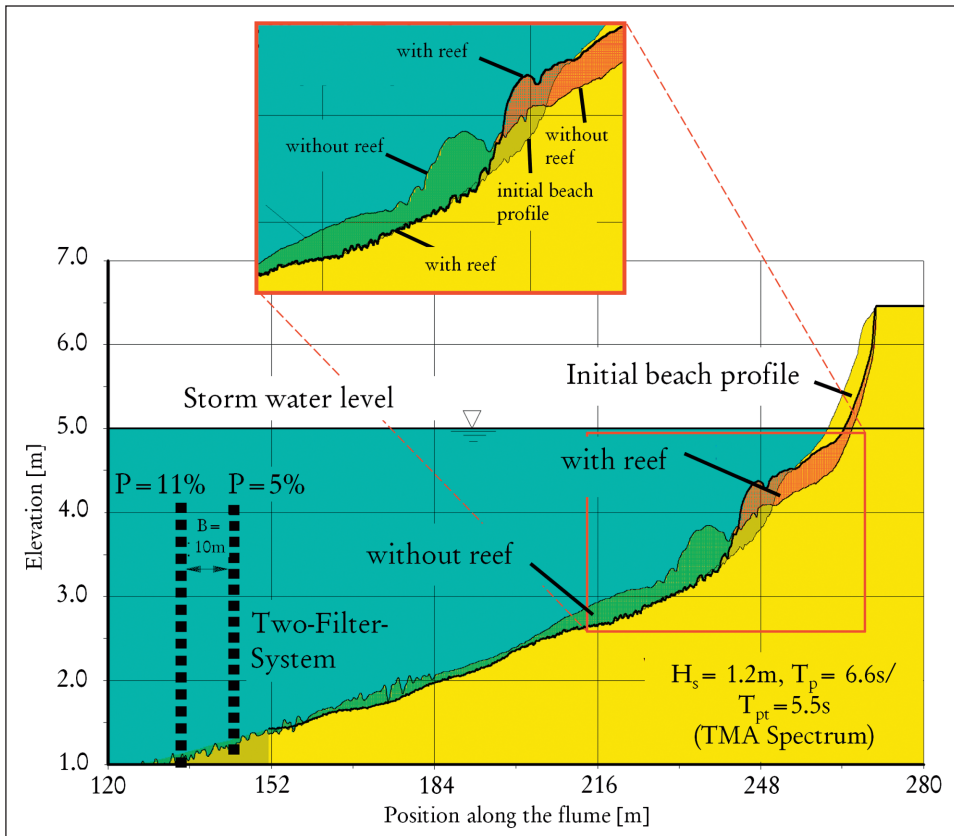


Fig. 21: Beach profile after a storm with and without a reef (OUMERACI, 2010a)

Further results indeed show that the relative spacing B/L is much more relevant than the number and porosity of the filters regarding the control of the reflected, transmitted and dissipated wave energy. A more detailed discussion of these aspects is given by OUMERACI and KOETHER (2009); KOETHER and OUMERACI (2001), OUMERACI et al. (2001a); KOETHER et al. (2000) and KOETHER (2002).

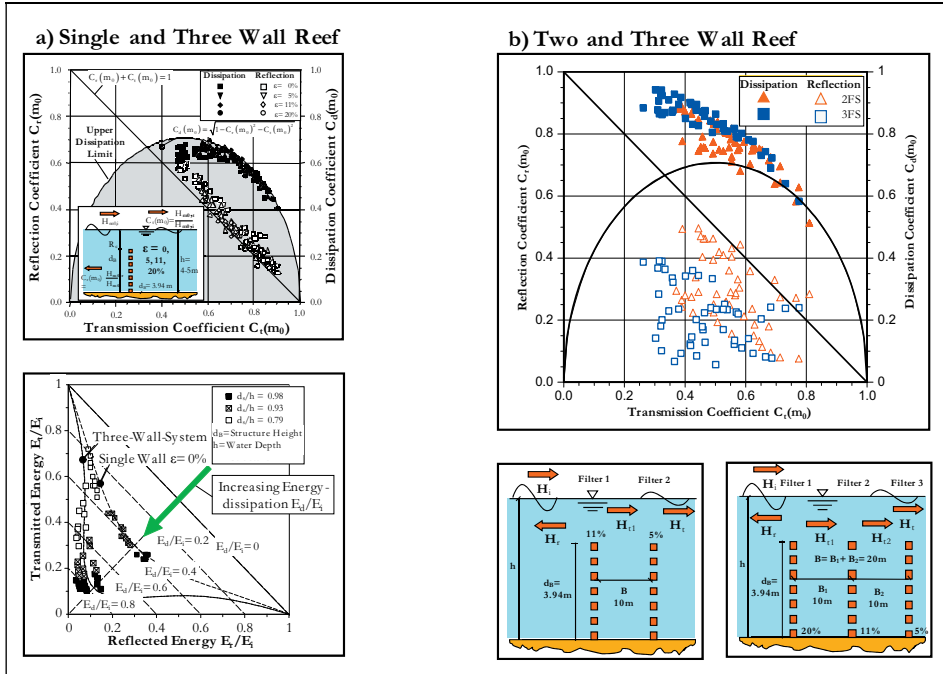


Fig. 22: Basic difference between the hydraulic functioning of a single-wall reef and a submerged wave absorber (OUMERACI and KOETHER, 2009)

This second case study again shows that substantial improvements to existing concepts can only be achieved through a better insight into the mechanisms and processes that govern hydraulic performance. In fact, using a single submerged screen, only a very limited amount of incident wave energy can be dissipated, i.e. a decrease in wave transmission can only be achieved at the cost of an increase in wave reflection (see OUMERACI and KOETHER, 2009 for more results).

Using a conventional reef made of rubble material would require a very wide structure and a progressive decrease of porosity in the wave direction in order to achieve satisfactory wave-damping performance. This would not only be costly and difficult to construct and maintain, but would also make it very difficult to control hydraulic performance by varying structural parameters, as is the case in this new artificial reef concept.

An understanding of the underlying mechanisms has shown that a new reef concept consisting of two or three submerged thin filters is an elegant and cost-effective alternative to overcome most of the drawbacks of existing reef concepts, including a substantial reduction and improved control of the reflected and transmitted components of the incident wave energy by varying structural parameters (submergence depth, porosity, number and spacing of submerged slit walls.) A theoretical model to optimise submerged wave absorbers has been developed by KOETHER (2002). This model has been successfully validated by large-scale experimental data for regular and irregular waves as well as for submerged single-slit walls and wave absorbers with two and three filters.

Preliminary tests in the Large Wave Flume (GWK) on a single-wall as well as a two- and three-wall submerged wave absorber subject to one meter high solitary waves have shown that this reef concept might also be applied to provide protection against tsunamis (OUMERACI, 2006). In fact, the proportion of wave energy of the incident solitary waves dissipated is greater than 75 % and 85 % for a two-wall and a three-wall system, respectively. The experimental results showing the incident, reflected and transmitted waves for a single-, two- and three-wall system are plotted and discussed in OUMERACI and KOETHER (2009). In overall terms, the results obtained in the GWK have shown that submerged wave absorbers may in principle provide a tailor-made solution to shore protection. However, their practical implementation at a specific site will require further considerations, such as survivability on a highly energetic sandy coast, local morphological changes, the effect of tides, etc.

(c) High-Mound Composite Breakwater (HMCB)

The concept of an HMBC was first applied in practice in 1830 in Cherbourg, France, and later in 1890 in Alderney, UK. Based on this original concept, a new HMCB concept (Fig. 19c) has recently been extensively tested in the GWK (Fig. 23b; c) within the framework of two joint research projects carried out by the Leichtweiß-Institute (LWI) in collaboration with the Port and Harbour Research Institute (PHRI), Yokosuka, Japan and the Civil Engineering Research Institute (CERI), Sapporo, Japan.

The new HMCB concept was intended to be applied mainly as a sea wall for protecting artificial islands (offshore airport) and roads with heavy traffic along the coast as well as a harbour breakwater. The major characteristic of the HMCB concept is to cause the highest waves in the spectrum to break before reaching the crest structure by means of a relatively flat slope (about 1 : 3). This concept has the following advantages: (i) the required amount of rubble material is much less than for a conventional rubble-mound breakwater, (ii) the required armour units are smaller since they are all placed below the still water level and (iii) the required crest structure is much smaller than a conventional caisson breakwater.

In order to further substantially reduce breaking-wave impact loads on the superstructure and to overcome further drawbacks of the old HMCB concept (excessive wave reflection, overtopping, spray generation, etc.), a major innovation was introduced to improve the performance of the concrete superstructure. This involves the addition of a slit wall made of piles (porosity of about 30 %) in front of the structure and a relatively short dissipation chamber behind it. If a breaking wave reaches the structure, the total wave force is split spatially and temporally into the following force components (see Fig. 19c): (i) a force component on the permeable front wall, (ii) a force component on the impermeable back wall and (iii) a stabilizing downward force on the bottom slab of the dissipation chamber.

In addition to a reduction of wave loads and the subsequent reduction of the required size of the concrete superstructure, a significant improvement of the overall hydraulic performance characteristics is also achieved by applying the new HMCB concept. The improvements in comparison to the older concept (vertical impermeable superstructure) based on extensive large-scale model investigations in the GWK (Fig. 23b; c) are given in Fig. 23d.

With regard to wave loads, it is seen that the achieved reduction of the horizontal and uplift forces would result in a reduction of about 50 % of the weight of the superstructure necessary to ensure sliding stability. With regard to hydraulic performance, it is seen that

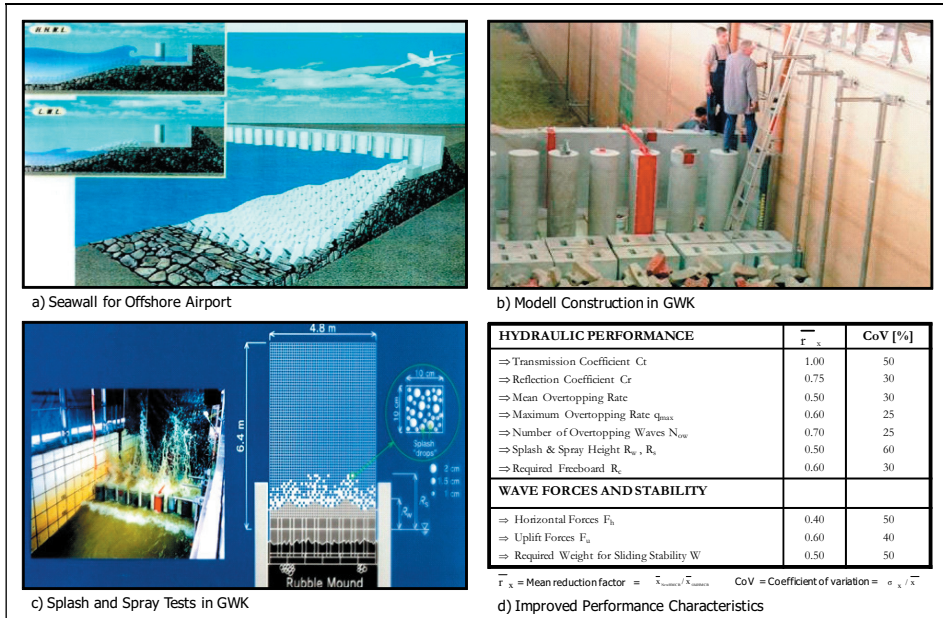


Fig. 23: High-Mound Composite Breakwater Concept (HMCB)

wave reflection is reduced by about 25 %, and as a result of the reduction in wave overtopping, the required crest level above still water level is reduced by about 40 %. Even without the installation of splash reducers along the front and back walls of the concrete superstructure, the splash/spray heights are reduced by half. Further details concerning the results shown in Fig. 5 are given by OUMERACI and MUTTRAY (1997); MUTTRAY et al. (1998); OUMERACI et al. (1998); TAKAHASHI et al. (2000); SCHÜTTRUMPF et al. (2000); MUTTRAY et al. (2000) and OUMERACI et al. (2000b). The HMCB concept has recently been implemented in Mori Harbour, Hokkaido (MORI et al., 2008).

It is also worth noting that the reduction of spray generation along wave damping structures is becoming an increasingly important design requirement, particularly when the structures are intended for the protection of offshore airports, littoral roads with heavy traffic, etc. The growing importance of this relatively recent aspect may be explained by the detrimental effects that spray might have on inland and near-shore infrastructures, operations and vegetation, etc. In fact, spray can be transported by wind up to 30 km inland and the flux of spray salt can attain values of up to 400 $\mu\text{g}/\text{m}^2\cdot\text{s}$. Large quantities of salt water dispersed over wide coastal areas may result in the following: (i) short term detrimental effects such as disturbance/stoppage of car traffic (KIMURA et al., 2000), electric power supply, port and airport operations; (ii) longer term impacts such as salt corrosion of buildings and other facilities, damage to agriculture and inland vegetation, etc.

One of the most challenging tasks to cope with salt spray is therefore the development of innovative shapes of the structure crest so as to substantially reduce the splash/spray height caused by wave-breaking. For this purpose, special tests in the GWK (Fig. 23c) were

The relatively low crest level and the discontinuous nature of the barrier resulted from the requirements that tourists on the promenade should continue to enjoy an unobstructed view of the sea and also retain direct access to the beach. Moreover, the barrier should architecturally and aesthetically fit into the local landscape, i.e. it should not appear to be a coastal protection structure on first sight (Fig. 25a). The efficiency of the OWBD concept in terms of wave overtopping reduction was successfully tested in the Large Wave Flume (GWK) in Hanover (Fig. 25b; c) and subsequently implemented on Norderney (Fig. 25d), where it has withstood many storm surges without damage for more than 5 years.

Because broadening of the embankment crest was not practically feasible, the OWBD concept proved to perform best in reducing wave overtopping (by a factor of 5) compared to other conventional alternatives. More details on the results can be found in OUMERACI et al. (2000c) and SCHÜTTRUMPF et al. (2002).

This large-scale model case study in the GWK has shown that under certain circumstances, storm waves can be damped effectively by a discontinuous low barrier made of aesthetically and functionally well-conceived wall elements. Using a much wider barrier and more robust wall elements, this concept may probably also be applied to provide protection against tsunamis (OUMERACI, 2006).



Fig. 25: Onshore Wave-Damping Barrier (OWDB)

In fact, evidence in the field concerning sea walls and breakwaters during the 2004 Indian Ocean Tsunami clearly suggests that protective structures should not be designed to completely halt a tsunami wave. Indeed, this is neither economically justifiable nor environmentally and socially acceptable. Protective structures for this purpose should thus preferably (i) aim at progressively weakening the power of a tsunami without completely blocking inundation and (ii) have the overall additional benefit of broadly blocking floating debris in a less abrupt manner. Such a concept would be especially appropriate for protecting urbanized

coastal areas and tourist resorts. This particularly applies to areas where forests (bio-shields) cannot be planted and must therefore be replaced by man-made barriers that blend well with the local marine landscape in architectural terms (OUMERACI, 2006).

3.4 Wave-induced flow on and within rubble mound breakwaters

Generally speaking, the hydraulic stability of armour units can be studied with sufficient engineering accuracy using commonly implemented small-scale models. In order to realise reliable breakwater design it is not only necessary to ensure structural integrity of the armour units, but also important to have a good knowledge of: (i) the internal flow field and its interaction with the external flow; (ii) the wave fields in front of and behind the breakwater, which both largely depend on the internal flow behaviour; (iii) the wave energy dissipated within each layer of the breakwater; (iv) the uplift pressure on the crown wall, which is determined by the non-saturated internal flow field in the upper region of the core material (OUMERACI and PARTENSKY, 1991).

Due to the serious scale effects associated with the internal flow, small-scale model testing is inappropriate, which means that the use of large-wave facilities is indispensable. For this reason, a research strategy was developed to systematically investigate the hydraulic processes that occur in the five domains presented in Fig. 26 using the Large Wave Flume (GWK). These include: (i) the wave field at the structure toe (domain 1), (ii) wave runoff and rundown on the seaward slope (domain 2), (iii) the flow field and the wave damping inside the breakwater (domains 3 and 4) and (iv) wave transmission behind the breakwater (domain 5).

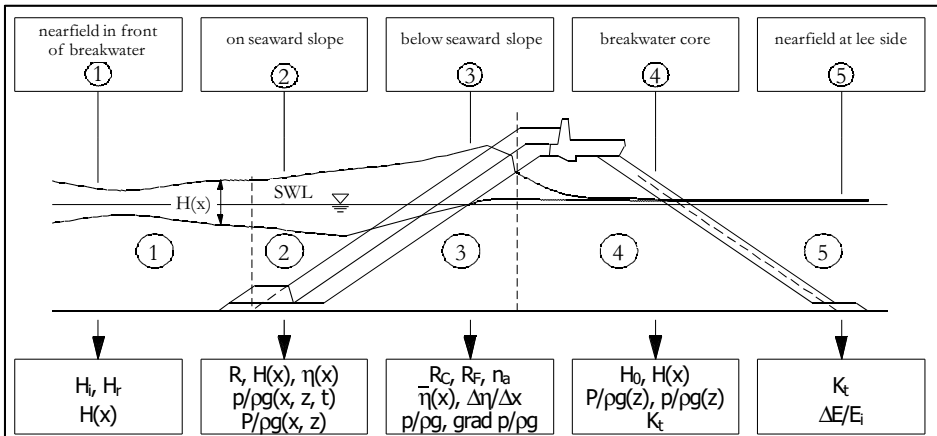


Fig. 26: Research strategy for rubble-mound breakwaters in the Large Wave Flume (GWK)

The experimental setup used for this purpose is shown in Fig. 27. The Reynolds number related to the grain size of the core material (crushed stone with $d_{50} \approx 4$ cm) was larger than 105. The sublayer is made of crushed stone with $d_{50} = 12$ cm, whereas the armour layer is composed of 40 kg Accropodes. Water depths in the flume during the tests ranged between

3.5 m and 4.9 m. Regular waves with heights of up to $H = 1.8$ m and periods of up to $T = 10$ s as well as irregular waves with $H_s = 0.2-1.2$ m and $T_p = 2-10$ s were generated.

As shown in Fig. 27, a total of 30 wave gauges were used. These included three runup gauges on the slope of the armour layer, the sublayer and the core as well as five wave gauges to measure internal water level fluctuations. In order to measure the wave pressure along the boundaries of the different layers and the pore pressure inside the core, a total of 34 pressure transducers was installed. More details of these measurement techniques are given by MUTTRAY (2000). The measuring devices outside, along and within the breakwater were located in such a way that the internal flow field could be easily determined as a function of the incident wave motion for any wave phase (Figs. 27; 28).

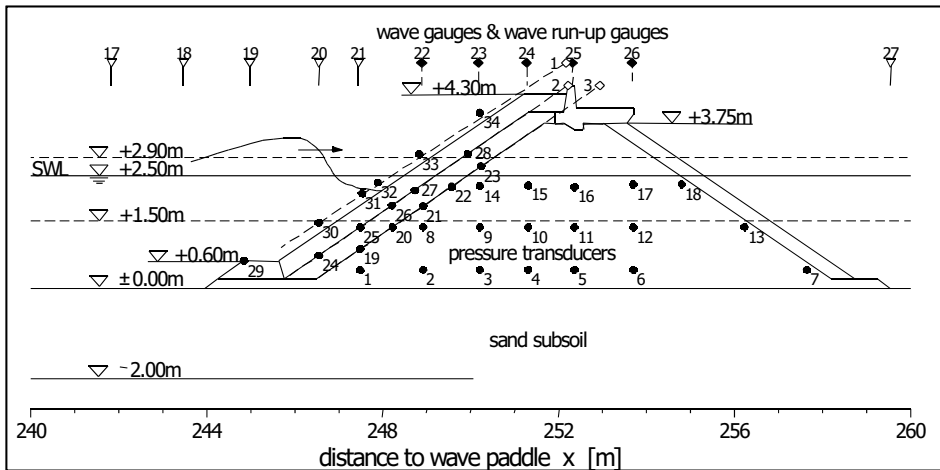


Fig. 27: Locations of measuring devices outside, along and within the breakwater in the GWK model (MUTTRAY and OUMERACI, 2005)

Based on the research strategy and the experimental setup shown in Figs. 26; 27, respectively, new results and formulae were derived for each of the five domains shown in Fig. 26: (i) Domain 1: full description of the partial wave field in front of the breakwater, including wave transformation on the foreshore ($H(x)$), wave asymmetry and phase shift between the incident (H_i) and reflected (H_r) waves; (ii) Domain 2: runup and rundown (R), water level fluctuations $\eta(x)$ and wave height development ($H(x)$) on the breakwater slope as well as within the structure, pressure distribution along the slope as well as wave energy dissipation along and within the structure; (iii) Domain 3: maximum setup and set-down along and within the structure, runup within each layer, inflow and outflow, air entrainment into the breakwater core, internal wave breaking, pore pressure distribution in the breakwater; (iv) Domain 4: development of wave spectra in the core, wave damping ($H(x)$), wave transmission into the core, vertical and horizontal pore-pressure distributions, wave length inside the breakwater; (v) Domain 5: wave transmission and wave spectra on the lee side of the breakwater.

For more details of the newly-developed formulae to describe the afore-mentioned processes occurring in the five domains, reference should be made to the PhD thesis of MUTTRAY (2000). Only two examples are provided below to illustrate these processes, which

cannot be properly reproduced in commonly applied small-scale models and must therefore be investigated by means of large-scale model tests. The first example concerns the evaluation of wave energy dissipation along and within the breakwater, as shown in Fig. 29.

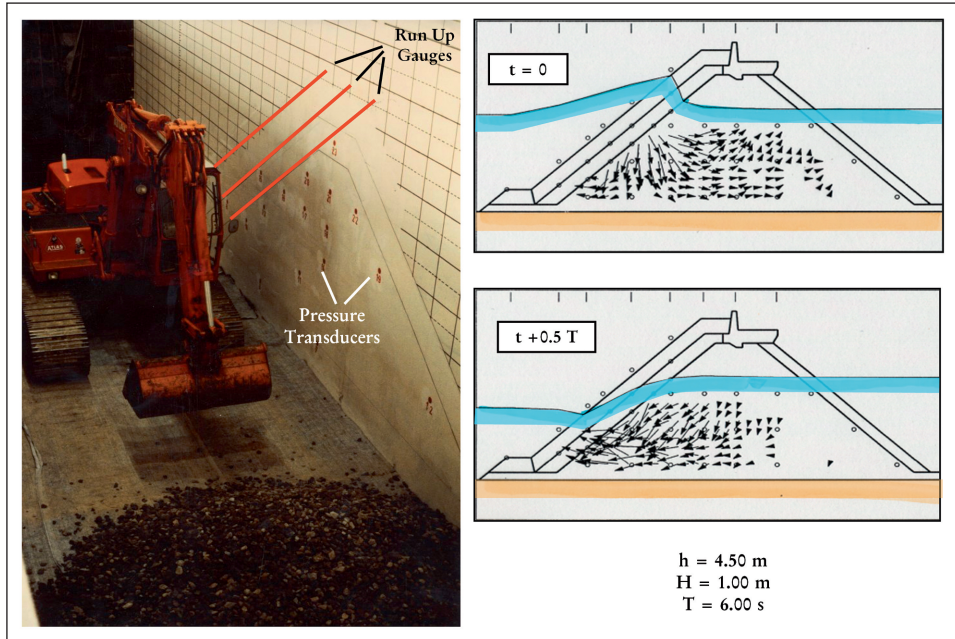


Fig. 28: Model construction in the GWK and the flow field determined for maximum wave run-up and run-down

The relative contributions of each layer to the overall energy dissipation can also be determined. It has been shown that the energy dissipation must be calculated from the difference between the energy flux of the partial standing waves in front of the breakwater and that of the transmitted waves on the leeward side. This leads to the dissipated energy ΔE in relation to the incident wave energy E_i :

$$\frac{\Delta E}{E_i} = (1 - K_r)^2 - K_t^2 \quad (1)$$

as opposed to the commonly-used formula $\Delta E/E_i = 1 - (K_r^2 + K_t^2)$, which assumes linear superposition of the incident and reflected (progressive) waves and is thus only valid for reflection coefficients of $K_r = 0$ and $K_r = 1$. This is not the case for the partial standing-wave field that actually exists in front of a rubble mound structure. In Eq. (1), K_r and K_t are the reflection and transmission coefficients, respectively. The results of the investigation show that, of the total incident wave energy, the transmitted wave energy amounts to less than 1 %, the energy of the partial standing waves in front of the breakwater varies between 10 % and 65 %, while the dissipated energy lies between 9 % and 65 %.

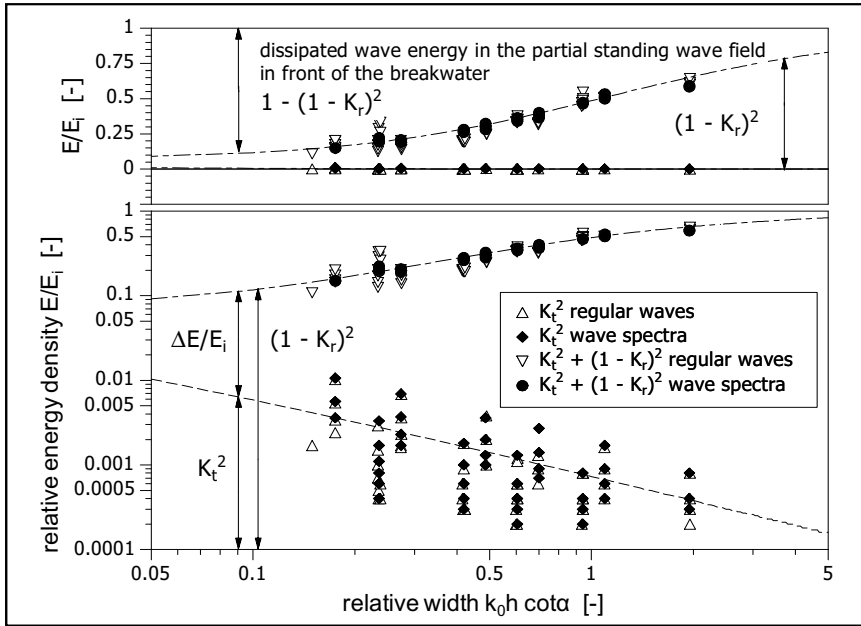


Fig. 29: Wave energy dissipation along and within the breakwater (MUTTRAY and OUMERACI, 2005)

The second example concerns the wave-induced pore pressure distribution within the breakwater. Based on detailed measurements of pore pressure and internal water level fluctuations (Figs. 27; 28), new formulae have been derived to describe the internal pressure field as a function of the incident wave parameters. An example of this is shown in Fig. 30 for $H = 1.06$ m, $T = 5$ s and a water depth at the toe of $h = 2.49$ m. It may be the case that in the two first layers of the breakwater the pressure gradients are very high and internal wave breaking occurs. The internal flow field can be calculated from the isolines of the pressure gradients (see Fig. 28).

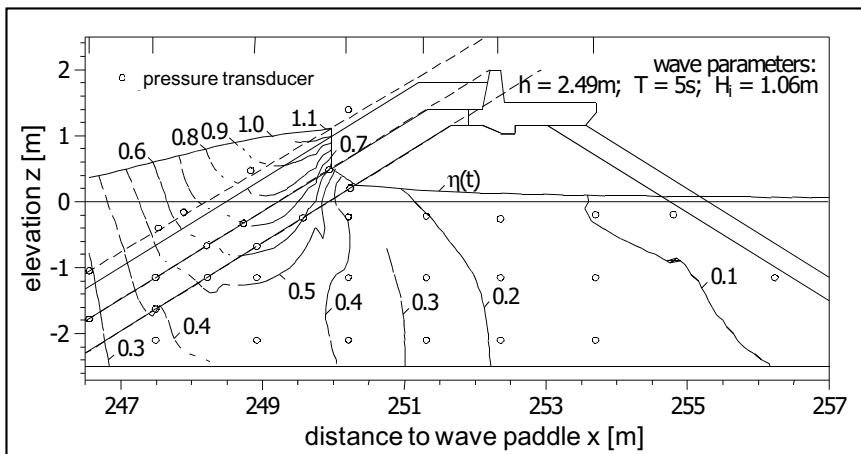


Fig. 30: Wave-induced pore pressure field (MUTTRAY and OUMERACI, 2005)

3.5 Hydraulic stability/performance of coastal protection structures made of geotextiles

Geotextile containments are mostly applied in coastal engineering to prevent erosion and stabilize beach-dune systems during storm surges. For this purpose, different types of containments have been implemented, very often as a last line of defence in combination with beach nourishment. Because the deformations of geotextile containments strongly affect hydraulic stability (e.g. SAATHOFF et al., 2007; OUMERACI and RECIO, 2010) and since the modelling of these deformations is influenced by scale effects, large-scale tests offer the sole alternative for reliably quantifying the hydraulic stability of geotextile structures under wave attack.

An impressive example of such a last line of defence behind a beach nourishment area is the wrapped sand containment needle-punched composite geotextile (woven PP slit film and non-woven PET). This method was used to reinforce a dune on the island of Sylt (North Sea, Germany), as shown in Fig. 31. The stability of this stepped barrier was tested successfully in the Large Wave Flume (GWK). The latter survived several storm surges with water levels of about 2.5 m above mean water level and wave heights of up to 5 m. The fact that only the sand cover was removed confirms that the nickname “Bulletproof Vest” commonly given to this type of construction is appropriate. Further details of the design and construction of this shore protection installation are given by NICKELS and HEERTEN (2000).

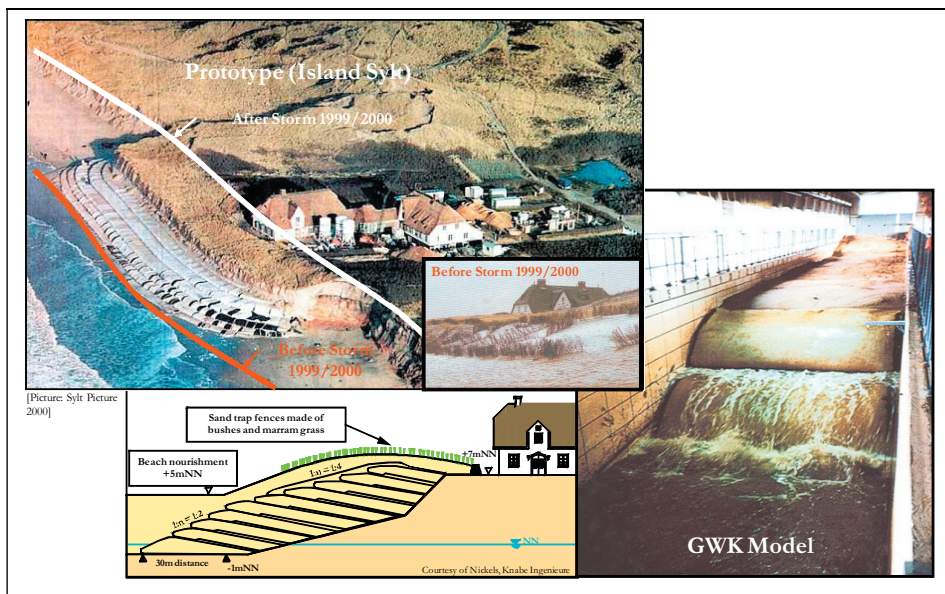


Fig. 31: Geotextile containment for dune reinforcement, Sylt/Germany (extended and modified from NICKELS and HEERTEN, 2000 in OUMERACI and RECIO, 2010)

In the majority of such applications, however, geotextile sand containers (GSCs) of different sizes are implemented. In order to study the failure mechanisms and hydraulic stability of GSCs under severe wave attack, it was thus decided to carry out large-scale tests in the GWK. Due to the different wave loads and boundary conditions that prevail on the slopes

and crests of such coastal protection structures, different stability behaviour and thus different stability formulae are to be expected for containers on the slope and the crest. The following results are extracted from the research reports on two comprehensive laboratory studies, namely small-scale model tests performed in the wave flume of the Leichtweiß-Institute (LWI) involving 1-liter sand containers subject to random waves with heights of up to 20 cm and large-scale model tests in the GWK involving 150-liter sand containers subject to random waves with heights of up to 1.6 m (OUMERACI et al., 2002; OUMERACI et al., 2003). Only the results of the GWK tests on the stability of the slope containers are briefly summarized below. These results were subsequently used as a basis for further research within the framework of PhD theses (e.g. RECIO and OUMERACI, 2007; 2008; 2009a; 2009b). Further results can be found in OUMERACI et al. (2002), OUMERACI et al. (2003) and OUMERACI and RECIO (2010).

The sand containers on the slope, which are located around still water level, are repeatedly moved up and down by wave uprush and downrush over the slope. This leads to an incremental seaward displacement of the containers. This dislodgement/pull-out effect, as observed in the wave flume and in the field, is illustrated in Fig. 32b; c.

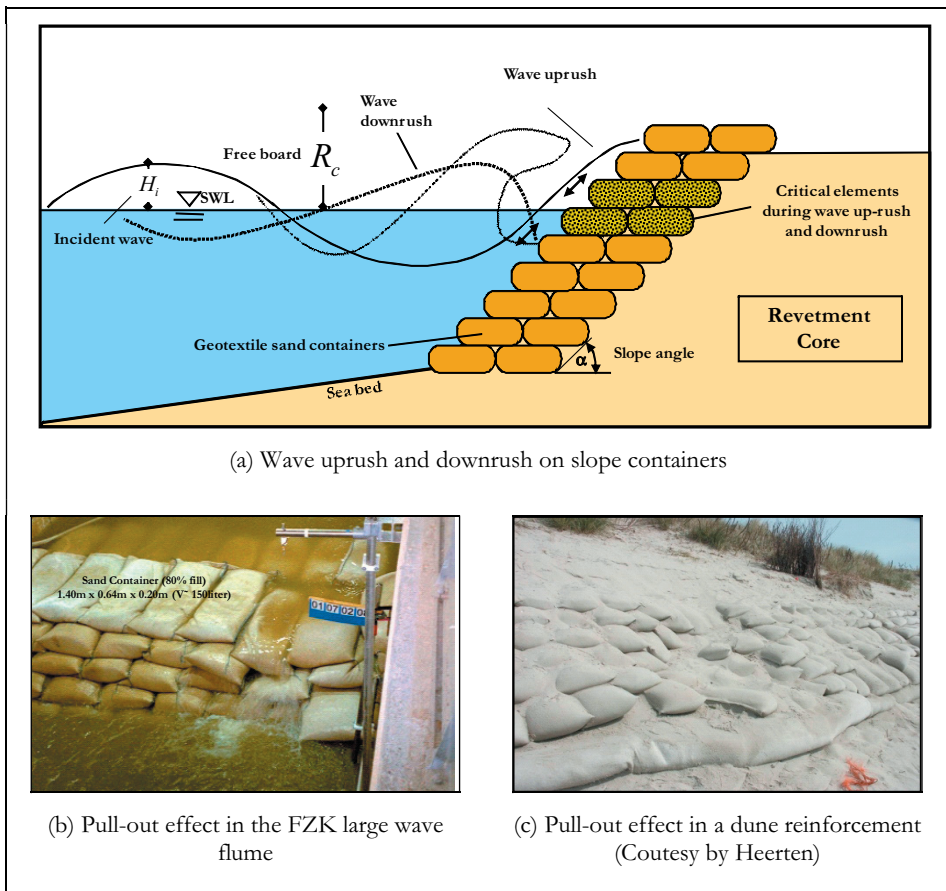


Fig. 32: Hydraulic failure modes of slope containers

Based on the HUDSON formula for the hydraulic stability of rock armour units, which is similarly to that of WOUTERS (1998), a stability number N_s is formulated and postulated as a function of the surf similarity parameter ζ_0 . This includes both the slope steepness $\tan \alpha$ and the wave parameters, significant wave height H_s and wave length L_{op} (Fig. 33):

$$N_s = \frac{H_s}{\left(\frac{\rho_E}{\rho_w} - 1 \right) \cdot D} = \frac{C_w}{\sqrt{\zeta_0}} \quad (2)$$

where the surf similarity parameter $\zeta_0 = \tan \alpha / \sqrt{H_s / L_{op}}$ is expressed in terms of the deep water length $L_{op} = gT_p^2/2\pi$ (T_p = peak period of wave spectrum). The following stability formula is thus obtained in terms of the characteristic size D of the container:

$$D = \frac{H_s^{3/4} \cdot T_p^{1/2} \cdot (\tan \alpha)^{1/2}}{C_w \cdot \left(\frac{2\pi}{d} \right)^{1/4} \left(\frac{\rho_E}{\rho_w} - 1 \right)} \quad (3)$$

Defining the characteristic size D as $D = l_c \cdot \sin \alpha$ according to the definition sketch shown in Fig. 33, Eq. (3) can be reformulated in terms of the length l_c of the slope containers to give:

$$l_c = \frac{H_s^{3/4} \cdot \sqrt{T_p}}{C_w \cdot \left(\frac{2\pi}{g} \right)^{1/4} \left(\frac{\rho_E}{\rho_w} - 1 \right) \sqrt{\frac{\sin 2\alpha}{2}}} \quad (4)$$

where H_s = significant wave height [m], T_p = peak period of waves [s]; α = slope angle of structure [°]; ρ_E = bulk density of the GSC [kg/m³]; ρ_w = density of water [kg/m³]; $\rho_E = (1-n) \cdot \rho_s + \rho_w \cdot n$ (with $\rho_E \approx 1800$ kg/m³ for sand); n = porosity of fill material [-]; ρ_s = density of grain material [kg/m³].

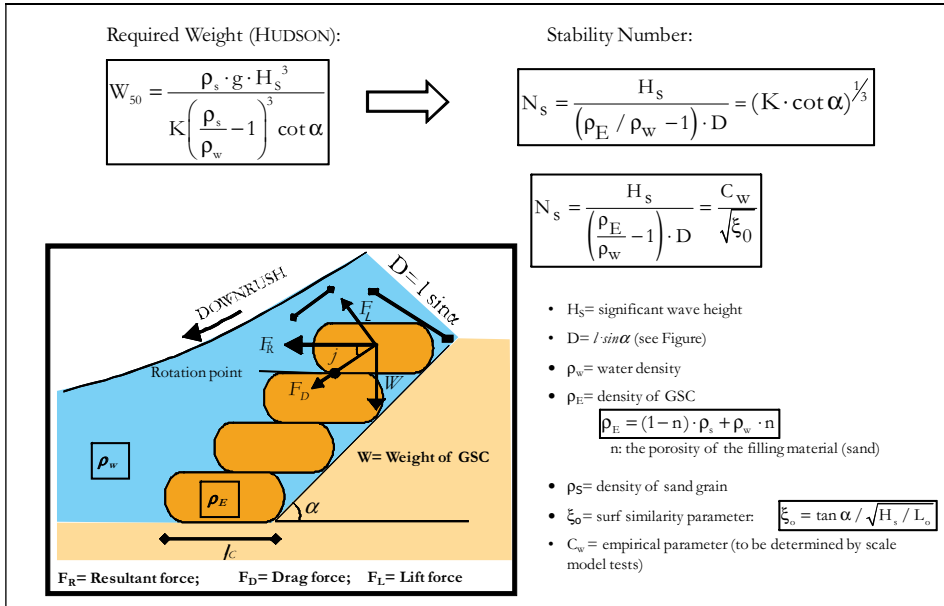


Fig. 33: Stability of slope containers based on the HUDSON formula

3.6 Effect of wave overtopping and breaching of sea dikes

The effects of wave overtopping are diverse and are highly dependent on the type of coastal structure under consideration and its usage, including the operations and installations on and behind the structure. In the case of a sea dike, for example, the possible failure modes due to overtopping flow are shown in Fig. 34a. These can in fact induce more dramatic effects, such as dike breaching initiated on the leeward side (Fig. 34b).

In fact, most of the dike breaches which occurred during the devastating storm surges of 1953 in the Netherlands and in 1962 in Germany were initiated on the leeward side by wave overtopping. Breach initiation by overtopping flow and breach growth still rank among the largest uncertainties when assessing flood wave propagation and its devastating effects on a protected area. Due to infiltration and other geo-hydrodynamic and soil dynamic factors involved, but also – even though to a lesser extent- to the possible scale effects associated with overtopping flow (SCHÜTTRUMPF, 2001), large-scale model tests were performed to determine the overtopping flow field and the failure modes as illustrated in Fig. 34a.

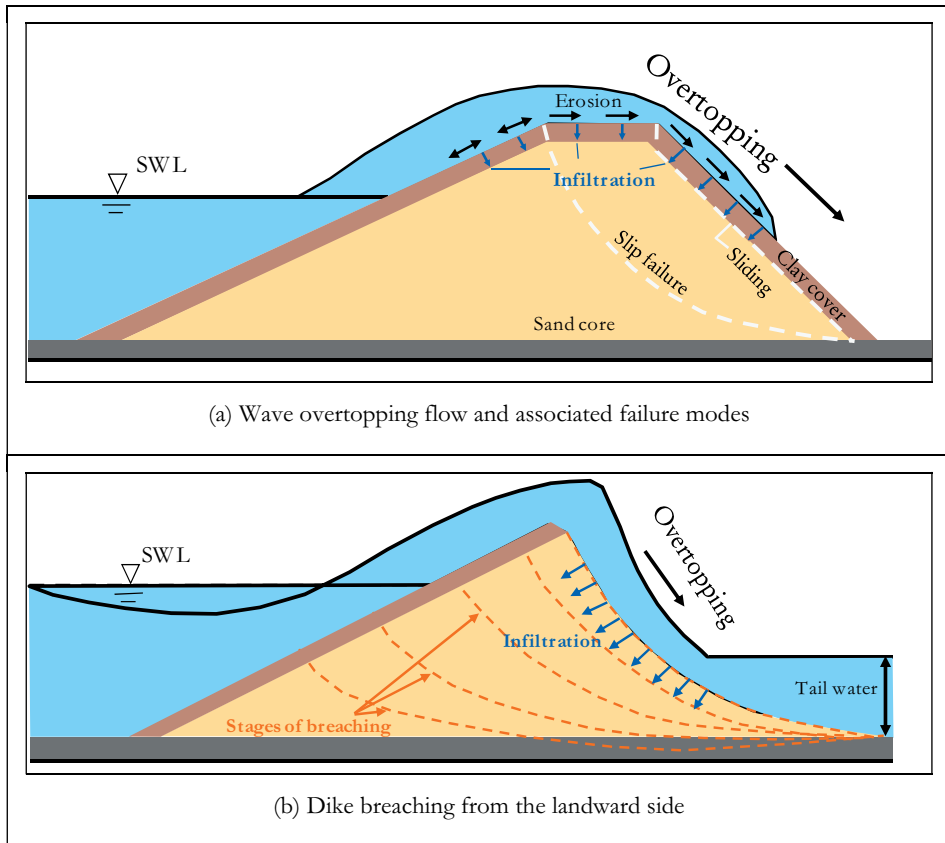


Fig. 34: Effect of wave overtopping on sea dike stability

Further large-scale tests were performed within the framework of the European FLOODsite project on the breaching of a typical North Sea dike consisting of a sandy core, a clay layer and a grass layer. Wave impacts and erosion on the seaward slope (Phase 1) as well as wave overtopping and erosion on the landward slope (Phase 2) were first investigated before commencing with Phase 3, which involves the initiation and development of a dike breach by excessive wave overtopping (Fig. 35).

The objectives of these tests were (i) to provide information concerning the influence of wave impact, wave overtopping and overflow on the initiation of breaching of sea dikes along the seaward and landward slopes; (ii) to gain a better understanding of the failure modes and breach growth of sea dikes as well as to analyse the associated hydraulic and hydro-geotechnical processes and (iii) to provide data for improving and validating existing computer models (e.g. D'ELISO et al., 2007; TUAN and OUMERACI, 2010; 2011; STANCZAK and OUMERACI, 2012). Due to the difficulties of scaling the reinforcement effect of the clay cover by grass vegetation, a scale of about 1:1 was adopted. The grass layer was taken from an existing North Sea dike. The composition of this particular grass species, which was installed in the GWK (Fig. 36), corresponds to a grass mixture commonly used on North Sea dikes in Germany, the Netherlands and Denmark. The clay used for the test consisted of erosion-resistant mate-

rial, as recommended by the German EAK (2002) Guidelines. In order to simulate natural conditions, different types of weak spots were included on the seaward and landward slopes such as (i) pipes of different diameters from the surface to the sandy dike core to simulate the tunnels created by burrowing animals (e.g. *Oryctolagus cuniculus*); (ii) damaged areas of the grass layer with and without leaves and stubbles and (iii) transitions between the soil and the grass layer as well as possible concrete settings within and on the dike (e.g. stairs).

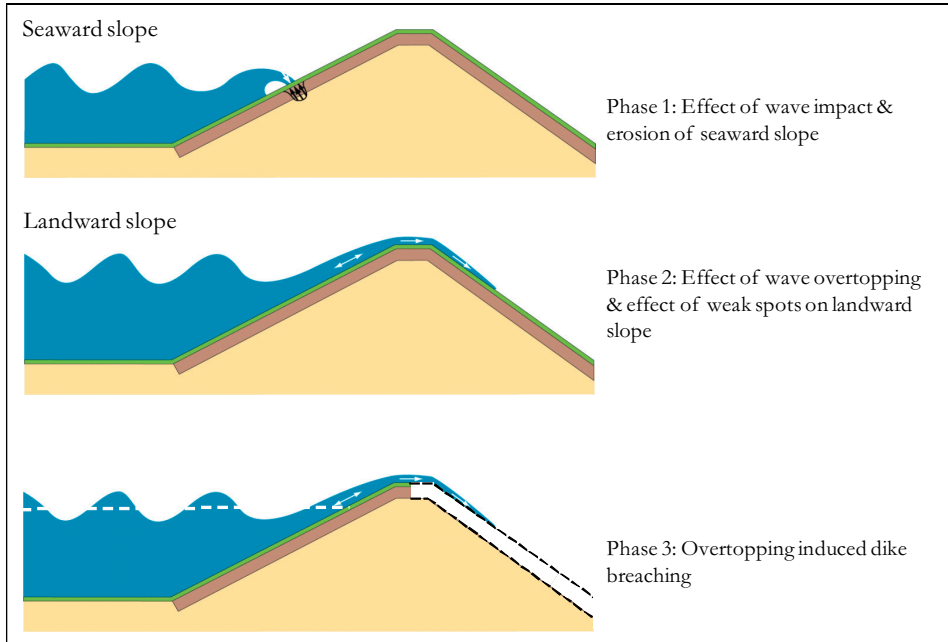


Fig. 35: Large-scale testing programme of sea dikes in the GWK



Fig. 36: Creating grass cover on the clay layer of a North Sea dike in the GWK

The following hydrodynamic and breach parameters were recorded: (i) wave parameters in the far field and the near field at the dike toe; (ii) pressures induced by different breaker types on the seaward slope and flow velocities on the dike surface (seaward slope, crest, landward slope); (iii) overtopping volumes; (iv) breach profile development. Soil parameters (e.g. moisture content) as well as grass-layer parameters were also measured. The main emphasis was placed on breach development, as shown in Fig. 37. Most of the results of these tests are reported by GEISENHAINER et al. (2007) and GEISENHAINER and OUMERACI (2008).



Fig. 37: Sea dike breach modelling in the GWK

Further interesting large-scale model tests on wave overtopping were performed at a scale of 1 : 2.75 for the rehabilitation of a historical seawall with a complex geometry built in 1858 to protect the Municipality of Norderney, Germany. Due to the variation of the height and location of the tidal ebb deltas 2 km offshore of the island, the seawall gradually became more exposed to wave action. The result of this was an increase in wave loading and overtopping. One of the main objectives of the tests was thus to investigate the wave overtopping performance of the seawall under these new wave exposure conditions and to propose suitable alternatives to reduce wave overtopping. The main results relating to the latter are summarized in Fig. 38, which illustrates the efficiency of six alternatives to reduce overtopping compared to Alternative 0 (existing situation).

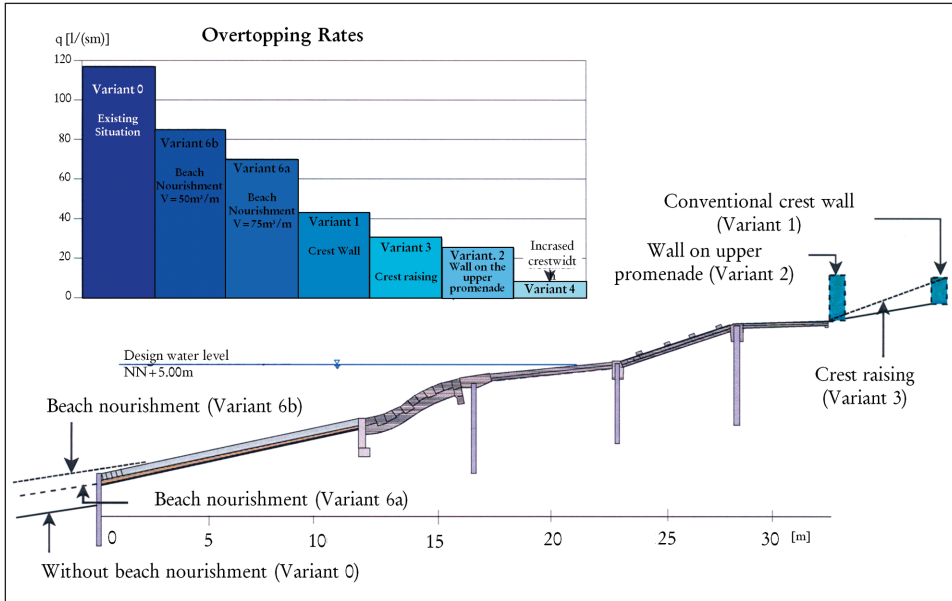


Fig. 38: Alternatives to reduce wave overtopping along the seawall of Norderney, Germany (OUMERACI et al., 2000b and SCHÜTTRUMPF et al., 2002)

3.7 Breaking-wave impact on slender pile structures

The proper simulation of wave breaking in deep water, generally caused by wave-wave interaction, and a correct reproduction of the resulting impact loads, are both very important factors for predicting extreme wave loads on offshore and other structures in deep water during storms. Due to the scale effects associated with air entrainment in breaking waves, impact loads can only be investigated adequately at a large scale. Using an empirical technique developed at the Technical University of Berlin based on so-called Gaussian wave packets, it is possible to generate focussed transient wave trains in the GWK (SCHMIDT-KOPPENHAGEN et al., 2004). These wave trains can focus at any selected location along the flume, thus resulting in a single breaking wave of up to about 3 m in height at that location. This technique permits much better control of the distance between the breaking point and the structure, and thus better control of the prevalent loading case. This is illustrated in Fig. 1 for the case of wave loading on a slender cylindrical pile ($D = 0.70$ m) based on tests in the GWK by WIENKE and OUMERACI (2005). By this means it was possible to more accurately reproduce and analyse each of the five loading cases shown by way of example in Fig. 39 for a vertical pile.

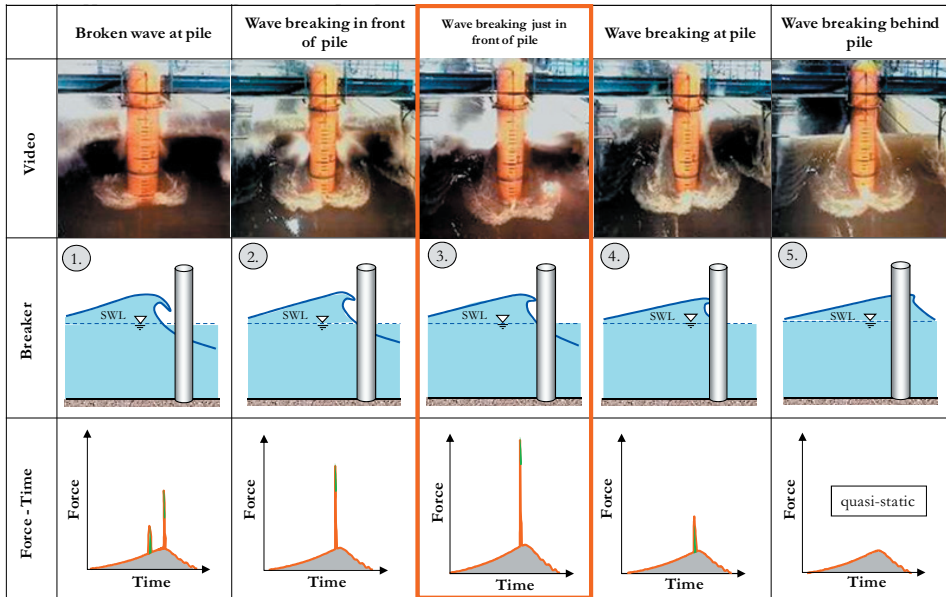


Fig. 39: Wave loading cases shown for the example of a vertical pile in the GWK

Moreover, the effect of pile inclination on the impact load was also investigated using the afore-mentioned focusing technique (Fig. 40). Based on systematic measurements in the Large Wave Flume (GWK) (waves and wave kinematics, wave pressure along and around the pile and total wave forces on the pile) as well as on simultaneous video recordings of wave-pile interaction, it was possible to gain a far better understanding of the wave impact on the pile. Further details of the measurement and analysis techniques are given by WIENKE (2001). Based on this improved understanding, it was possible to develop a theoretical formula for the 3-D impact loading of vertical and inclined piles which includes the curling factor as the sole empirical parameter (WIENKE and OUMERACI, 2005). The proposed loading formula has since been adopted in many international design standards (e.g. GL-GUIDELINES, 2005; ISO, 2007; ISO/IEC, 2009; GL-GUIDELINES, 2005, 2010). This research is still ongoing within the framework of a PhD thesis which mainly focuses on the impact loads generated by depth-limited wave-breaking and the pulsating wave loads caused by very steep near-breaking waves (IRSCHIK, 2012; IRSCHIK et al., 2002; 2004; 2010).

Extensive and systematic investigations were also performed in the GWK to determine the effect of neighbouring piles in different configurations (Fig. 41) on the wave loading of a single pile within a pile group with a given arrangement (e.g. tandem, side-by-side, staggered).

No reliable formula has yet been developed, however, to calculate the sheltering, interference and amplification effects of closely-spaced slender piles arranged in different constellations under breaking and non-breaking wave attack. The experimental programme consisted of 345 wave tests with a total of 15 different arrangements of the pile group (JUILFS, 2006; SPARBOOM and OUMERACI, 2006; HILDEBRANDT, 2006; HILDEBRANDT et al., 2008).

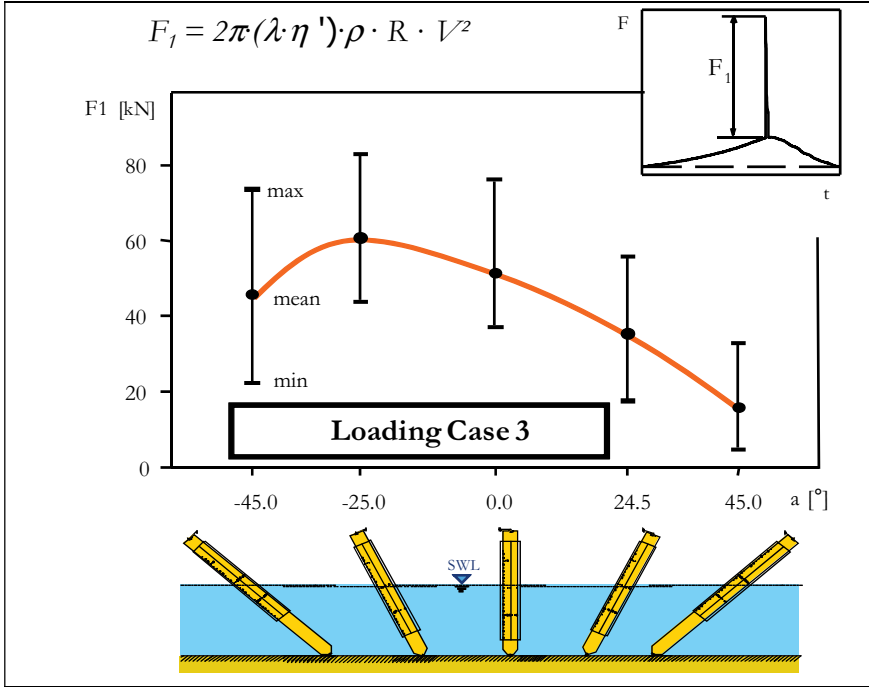


Fig. 40: Effect of pile inclination on the impact load as measured in the GWK (shown for the example of loading case 3)

Cylinder configurations	↓ waves ⊗ ⊕ D	↓ waves ⊙ ⊕ D ⊗ ⊕ D	↓ waves ⊕ ⊙ D ⊕ ⊙ D	↓ waves ⊙ ⊕ 3D ⊗ ⊕ 3D ⊙ ⊕ D
Loading case 1				
Loading case 2				
Loading case 3				

Fig. 41: Loading cases for selected pile group configurations in the GWK (adapted from JULFS, 2006)

Regular and irregular wave trains (H of up to 1.5 m and T of up to 8 s) as well as breaking waves generated by wave focusing were used in the tests. The pile of interest was instrumented by strain gauge transducers for measuring total wave loads. The wave kinematics were measured synchronously using several wave gauges and velocimeters (Fig. 42).

As shown in Fig. 40, the instrumented slender cylinder was installed as a cantilever pile attached to the support structure, which consisted of a robust steel frame equipped with a grid for the rapid fixation of other neighbouring piles in arranged in different constellations. It was possible to vary the spacing between the measuring cylinder and its neighbouring cylinders up to three times the cylinder diameter ($3 \times D$). A total of 15 basic configurations in tandem, side-by-side and in staggered arrangements was investigated.

Using this setup, it was possible to obtain detailed results of the synchronous time histories of water surface elevations and total wave loads as well as wave-induced horizontal and vertical components of both particle velocities and accelerations at the instrumented pile location (JUILFS, 2006; SPARBOOM and OUMERACI, 2006; HILDEBRANDT, 2006; HILDEBRANDT et al., 2008). These data are currently being analysed within the framework of a PhD thesis aimed at developing new simple formulae and a numerical model to predict wave loading on a single pile within a group of arbitrarily arranged piles.

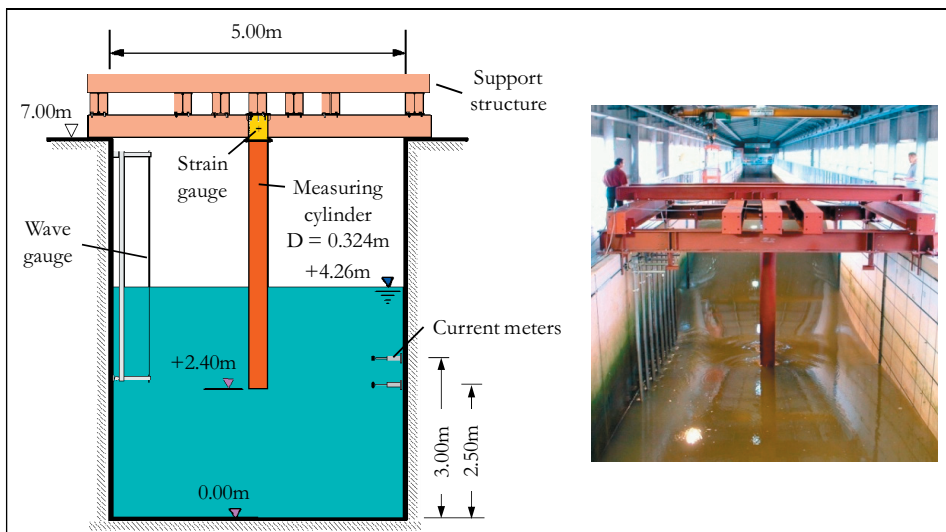


Fig. 42: Model setup with an instrumented cylinder (adapted from SPARBOOM and OUMERACI, 2006)

3.8 Wave-induced scour around marine structures and scour protection

The fact that wave-induced scour around slender piles has mainly been investigated in the past using small-scale models means that a high degree of uncertainty is attached to these test results owing to serious scale effects (e.g. OUMERACI, 1984; 1994b; HUGHES, 1993). Large-scale testing facilities are thus indispensable, particularly for investigating problems of this kind. In view of the foregoing, large-scale model tests were carried out in the GWK within

the framework of the EU-funded project Hydralab III (CoMIBBS) and a nationally-funded (BMU, Germany) project. Although both projects are aimed at investigating scour development, an additional aspect of the latter is to test different alternatives (made of rock material and geotextile sand containers) for the scour protection of monopile structures to support offshore wind turbines in the North Sea in water depths of $h = 20\text{--}30\text{ m}$ (OUMERACI et al., 2000a).

In order to study scour development over the entire duration of a storm, a variety of measuring and observation devices were deployed on and around a monopile in the model tests. These included wave gauges, Acoustic Doppler Velocimeters (ADV), a High Resolution (HR) Profiler, Faraday induction velocity meters (NSW), and Acoustic Backscatter Sonar devices (ABS, a high-resolution 3-D multi-beam sonar and a video camera placed inside the pile with a near-bed window (Fig. 43)). The deployment of various transducers to measure the wave and flow parameters in the vicinity of the pile was necessary owing to the high complexity of the flow around the cylinder induced by wave-pile interaction (see Fig. 44).

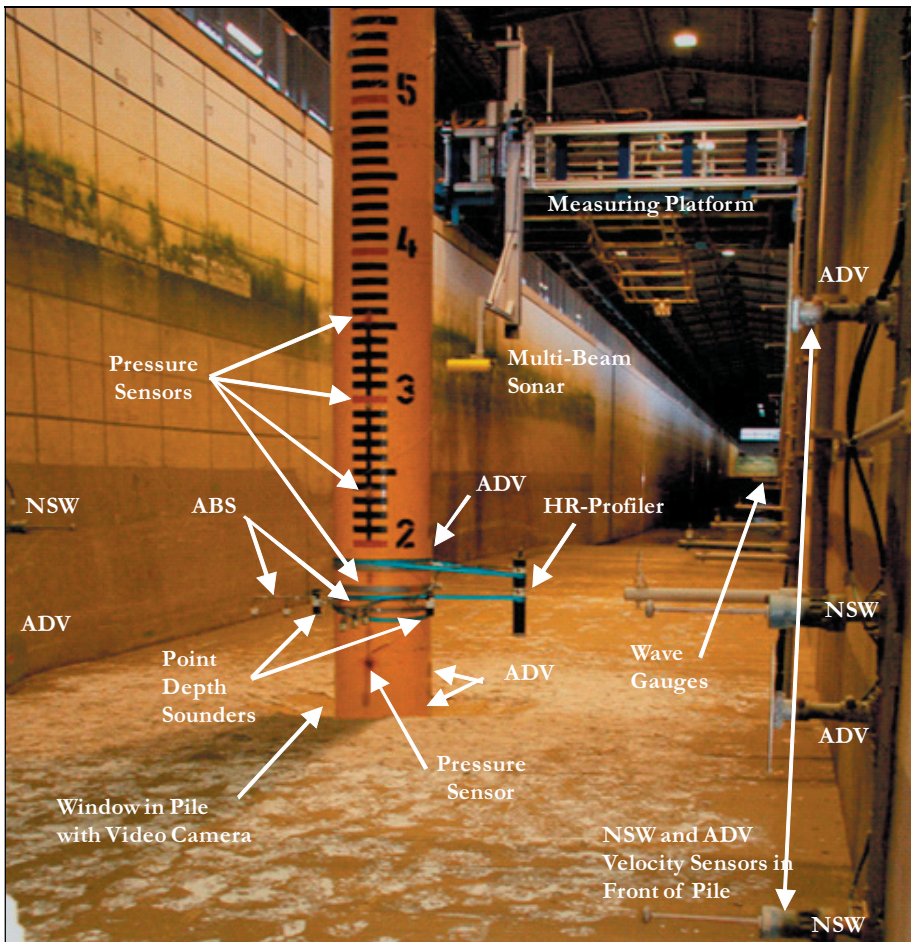


Fig. 43: Instrumentation on and around a slender monopile (GWK)

Example recordings of scour evolution under live bed conditions are depicted in Fig. 45.



Fig. 44: Complex flow induced by wave/pile interaction

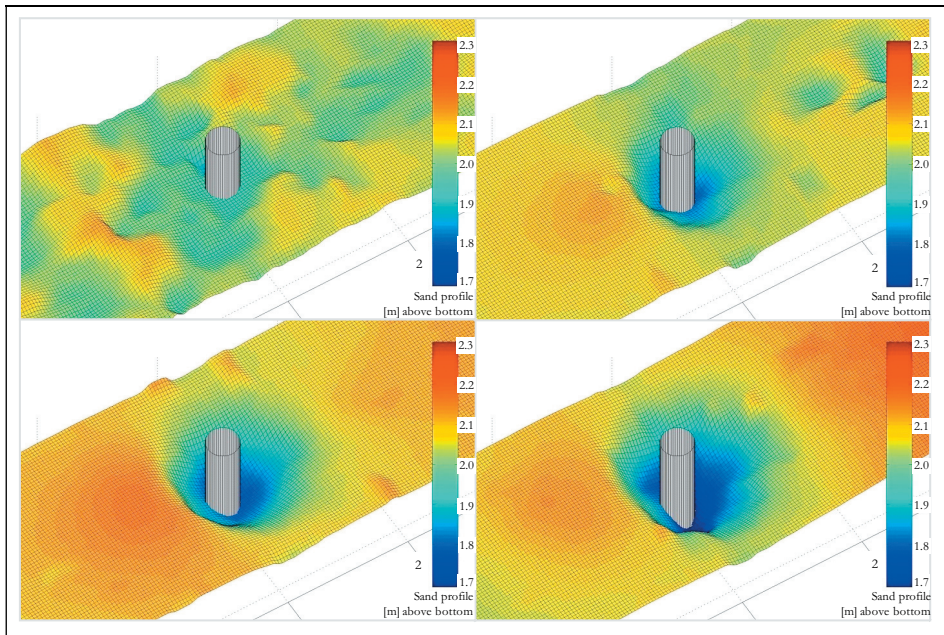


Fig. 45: Profiles of the sand bed for all test series (top left – test series 1 after 6000 waves, top right – test series 2 after 6000 waves, bottom left – test series 3 after 6000 waves, bottom right – test series 4 after 6500 waves) (adapted from PREPERNAU et al., 2008a; b; 2009)

From Fig. 45 it can be seen how quickly the scour hole deepens and widens with increasing duration of the storm (number of waves). The relative scour depth S/D based on measurements was found to increase exponentially with the Keulegan-Carpenter number KC , thus confirming qualitatively the exponential increase predicted by existing empirical formulae for wave-induced scour.

3.9 Sediment dynamics and beach/dune profile development under extreme storm surge conditions

The prediction of beach and dune profile development during storm surge conditions is important for the planning of protective counter-measures, which particularly include the optimisation of artificial beach nourishment as an environmentally acceptable method and the design of sand containers as a low-cost protection option. Suspended load, on the other hand, which constitutes the dominating material transport mechanism in the surf zone, is extremely difficult to predict owing to the high temporal and spatial variability of the hydrodynamic and morphodynamic processes involved. In addition, serious scale effects in modelling sediment transport do not permit quantitative conclusions to be drawn from the results obtained in tests using commonly implemented small-scale models (OUMERACI, 1994b; 1999; 2010c). In view of the afore-mentioned aspects, a large number of national and European research projects were carried out in the GWK, which permits the performance of experiments at near-prototype scale. An integrated experimental setup used to study the distribution of suspended sediment concentration over the water depth and along the entire surf zone is shown in Fig. 46 (DETTE et al., 1998a; b; PETERS, 2000).

Besides the efficient deployment of fixed measuring devices (27 wave gauges, 12 transducers for pore pressure, 2 NSW current meters), vertically as well as horizontally movable devices mounted on an instrument carrier (1 wave gauge, 3 ADV current meters, 6 OBS sensors and 1 ultra sonic backscatter profiler for sediment concentration and 1 bottom profiler) as well as a multi-beam sensor and other sensors were also used in the tests. A further important feature of the experimental setup shown in Fig. 46 is the bottom profiler mounted on a movable carriage equipped with a vertical instrument carrier (see Fig. 47).

After a comparative analysis of acoustic, optical, radar and mechanical sensors to monitor the submerged and exposed bottom profile, a decision was made to develop a mechanical system based on considerations of accuracy, robustness, reliability and accuracy (BEREND et al., 1997). The mechanical sensor shown in Fig. 47 can cope with bottom elevations ranging from 0 to 6 m and can operate under dry conditions (before and after tests) as well as underwater (during tests) with the same accuracy (± 10 mm). A PC installed on the movable carriage permits online visualization and an assessment of the accuracy of the ongoing data acquisition. The profiler can be used to monitor bottom and beach profiles as well as scour development in front of coastal structures.

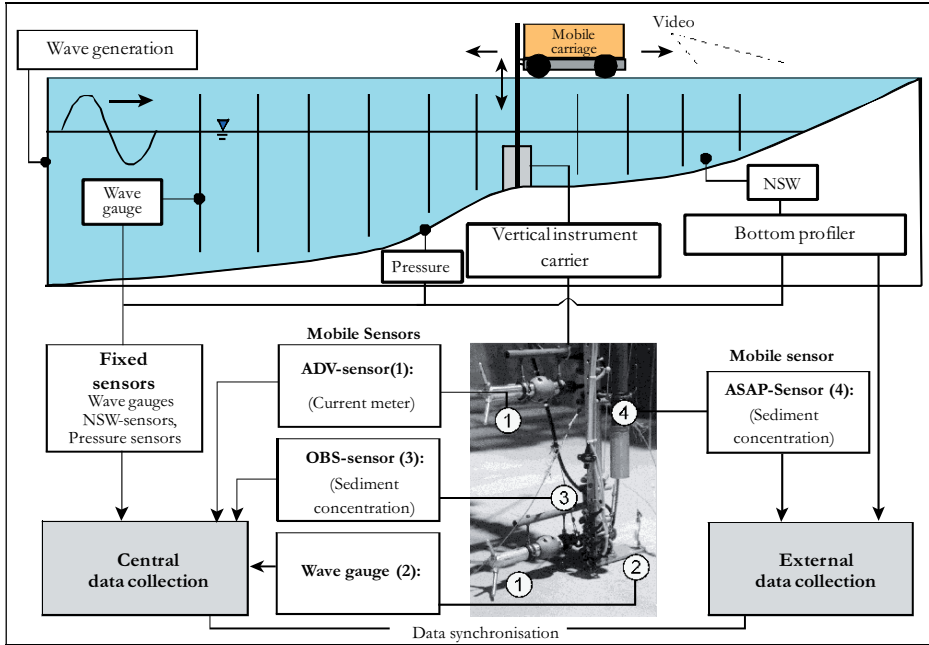


Fig. 46: Example of a setup and measurement strategy for beach/dune morphodynamic studies in the GWK (PETERS, 2000)

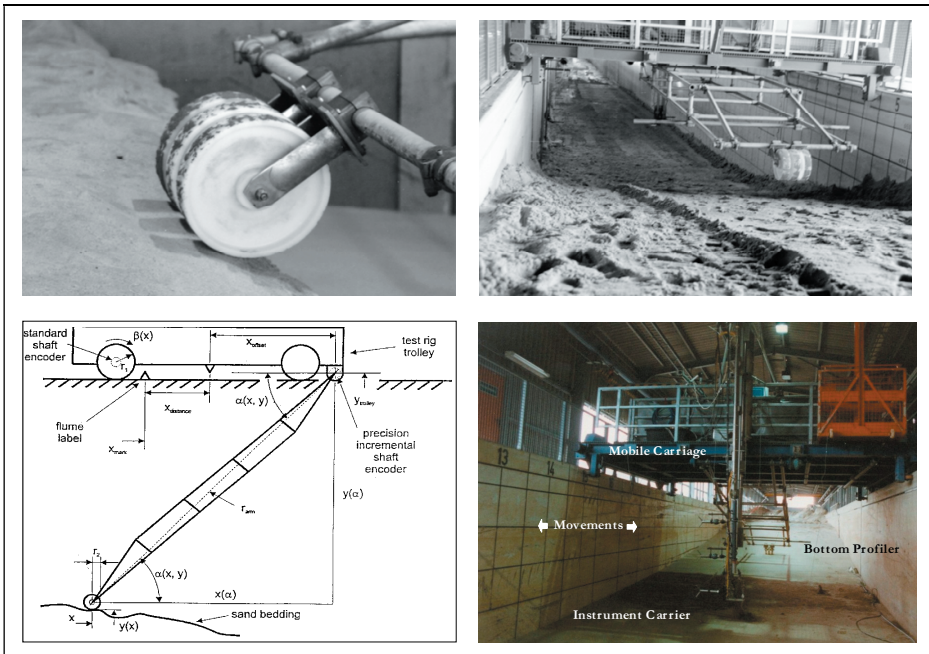


Fig. 47: Mechanical bottom profiler and moveable carriage (DETTE et al., 1998a; 1998b; BEREND et al., 1997)

Based on the measurement strategy shown in Fig. 46 and the innovative techniques used in the GWK, it was possible to optimise a number of artificial beach nourishment and other protection schemes for beaches and dunes for application in practice (DETTE et al., 1998a; 1998b). In addition, it was also possible to develop new formulae for suspended wave load and hydrodynamic processes in the surf zone within the scope of basic research projects (PETERS, 2000; NEWE, 2002; 2006). A methodology was also developed by NEWE (2002) for the large-scale model testing of beach/dune profile development under extreme storm surge conditions (Fig. 48). Based on a comparison with field measurements, NEWE also demonstrated that the most relevant transport mechanism during extreme storm surge events is cross-shore transport. This confirms the reliability of large wave flumes for predicting beach/dune profile development during extreme storm surges.



Fig. 48: Beach/dune profile development under extreme wave conditions in the GWK

A basic research project within the framework of a PhD thesis (AHMARI, 2012) has made extensive use of the large-scale model testing of suspended sediment under different wave regimes. A detailed comparative analysis of the results obtained using a multi-frequency Acoustic Backscattering Technique (ABS), an optical measurement technique (Optical Turbidity Meter) and a mechanical Transverse Suction System (TSS) has clearly shown that ABS is the most suitable technique for measuring sediment entrainment processes with sufficient temporal and spatial accuracy, especially above a rippled bed subject to both non-breaking and near-breaking waves (AHMARI et al., 2008 and AHMARI and OUMERACI, 2010; 2011). The suspended concentrations at different locations in the bed evolution time series beneath the ABS were combined to generate the images presented in Fig. 49, which shows an example of a time window of suspended sediment entrainment around a steep vortex ripple ($\eta_r/\lambda_r = 0.12$) beneath non-breaking weakly asymmetric regular waves ($H = 1.0$ m, $T = 5$ s, $h/L = 0.125$).

Fig. 49 also shows suspended sediment entrainment above a plane bed just before the point of wave-breaking of strongly asymmetric near-breaking regular waves ($H = 1.0$ m, $T = 5$ s, $h/L = 0.075$), including the horizontal orbital flow velocity u , measured in both cases by an Electromagnetic Current Meter (ECM) at 0.25 m above the undisturbed seabed (panels above SSC images in Fig. 49).

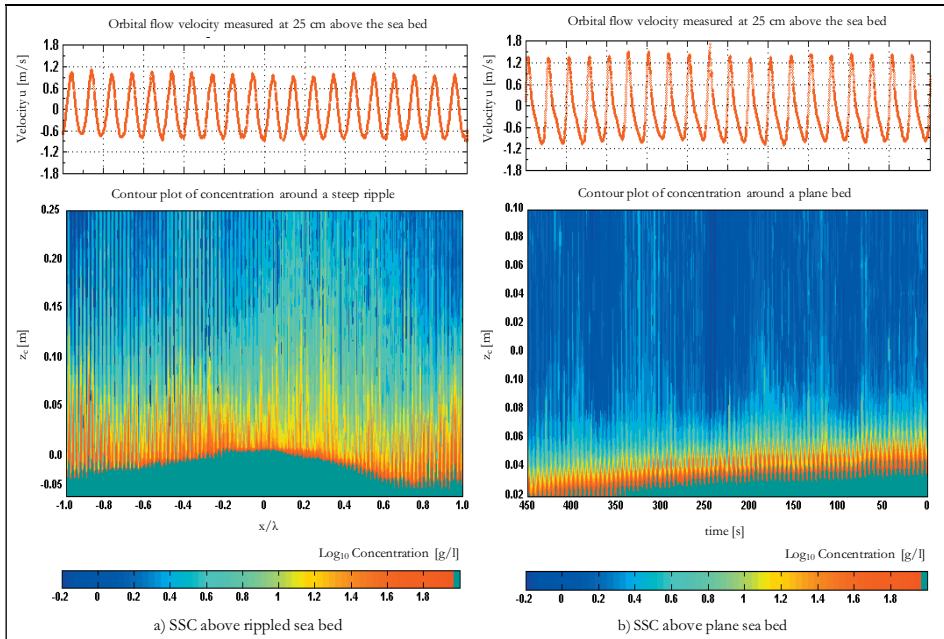


Fig. 49: Horizontal orbital flow velocity u , and Suspended Sediment Concentration (SSC), above (a) a steep ripple beneath non-breaking weakly asymmetric regular waves and (b) a plane bed beneath near-breaking strong asymmetric regular waves. (AHMARI and OUMERACI, 2011)

A further comparative analysis of suspended sediment entrainment above a rippled bed and a plane bed in both a low-energy and high-energy oscillatory flow regime was also performed, including the calculation and modelling of the sediment diffusivity profiles based on the ABS data set. The initial results of this analysis already appear to be promising. The analysis is still ongoing, and the results are expected to contribute significantly towards a better understanding of the temporal and spatial distribution of sediment entrainment processes above different seabed formations and under different wave-induced flow regimes.

4. Concluding remarks and perspectives

The experience gained over 20 years using the Large Wave Flume (GWK) has shown that large-scale model testing plays an important role in both basic and applied research. Moreover, it is an indispensable tool for investigating a range of hydraulic and geo-hydraulic processes in which serious scale effects are anticipated in the measurements performed in commonly implemented small-scale models (sediment transport and coastal morphodynamics, wave-induced flow in porous structures, wave impact loading of structures, etc.). The selected examples of applications have shown that such large-scale facilities are versatile and worth their value despite the various difficulties and high costs associated with their operation and maintenance. It is also important to stress the high relevance of management aspects, including a well-conceived planning of preparatory work supported by small-scale testing and numerical modelling.

As discussed in OUMERACI (1999), one of the most promising future modelling perspectives is to combine the synergetic effects of small-scale and large-scale modelling, together with numerical modelling and computations. The additional inclusion of field measurements for validation and verification purposes leads to what may be called “Composite Modelling”. As “Composite Modelling” is essentially based on the subdivision of a complex traditional overall physical model into several simple and easily repeatable process models which can be constructed at a large scale to minimize scale effects, it is expected that large-scale model testing will play an increasingly important role in the future (OUMERACI, 2010b).

A further step forward to minimize the laboratory effects associated with the 2-D character of existing large wave flumes and to permit the investigation of coastal hydrodynamic and morphodynamic processes along longer coastal sections with negligible scale effects is to construct large coastal engineering wave basins (water depths above 2.0 m, wave heights above 1.0 m, several hundred metres in length and more than 100 m in width). Such wave basins will also permit the generation of waves with oblique currents, including an effective sediment recycling system as well as a proper wind generation system. The next challenging task will be the introduction of biological and ecological factors for interactive modelling with waves, flow, sediment and structures in large-scale facilities.

5. Acknowledgements

The opportunity to prepare a paper summarising the author’s experiences using the GWK originated from an invitation to present a keynote lecture on these experiences at a workshop on December, 10, 2010 in Tainan, Taiwan to commemorate the 60th Anniversary of Tainan Hydraulic Laboratory (THL), which also has a similar large wave flume to the GWK. The author would therefore like to express his thank and appreciation to Professor HH Hwung for this opportunity. The present paper is an improved version of the one published in December 2010 in the proceedings of the afore-mentioned workshop. Most of the ideas and material presented herein are from completed research projects supported by the German Research Council (DFG), the Federal Ministry for Science, Education Research (BMBF), the European Community, German Coastal Authorities and industry. This financial support is gratefully acknowledged. Moreover, the contribution of the co-workers involved in these projects is also acknowledged.

6. References

- AHMARI, A.: Suspended sediment transport above rippled and plane seabed by non- and near breaking waves – A large scale laboratory study. PhD thesis submitted to TU Braunschweig, 2012.
- AHMARI, A.; GRUENE, J. and OUMERACI, H.: Large scale laboratory measurement of suspended sediment concentration induced by non-breaking waves with acoustic backscatter technique. Proc. 2nd International Conference on the Application of Physical Modelling to Port and Coastal Protection (CoastLab, Bari, Italy), 2008.
- AHMARI, A. and OUMERACI, H.: Measurement and analysis of the suspended sediment concentration by waves in a rippled bed regime. Proc. 9th International Conference on Coasts, Ports and Marine Structures (ICOPMAS, Teheran, Iran), 2010.
- AHMARI, A. and OUMERACI, H.: Measurement and analysis of near bed sediment processes by waves in rippled and plane bed regime. Proc. Coastal Sediment (CS, Miami, Florida, USA), 2011.
- ARCADIS: Polyurethane bonded aggregate revetments design manual. BASF Polyurethanes GmbH, 2010.
- BEREND, O.; SCHMIDT-KOPPENHAGEN, R. and DURSTHOFF, W.: Measurement of Sand Beach Profiles in the Large Wave Flume. Proc. 7th International Offshore and Polar Engineering Conference (ISOPE, Honolulu, Hawaii, USA), 1997.
- BERGMANN, H. and OUMERACI, H.: Wave loads at perforated caisson structures. Proc. 27th International Conference on Coastal Engineering (ICCE, Sydney, Australia), Vol. 2, 2000.
- BERGMANN, H.: Hydraulische Wirksamkeit und Seegangsbelastung senkrechter Wellenschutzbauwerke mit durchlässiger Front. PhD thesis, 2001.
- BERGMANN, H. and OUMERACI, H.: Digue innovante en caissons multi-chambres – Fonctionnement et sollicitations hydrauliques. Revue française de génie civil, Vol. 5, 7 (Spécial issue), 2001.
- BERGMANN, H. and OUMERACI, H.: Hydraulische Wirksamkeit und Wellenbelastung senkrechter Wellenschutzbauwerke mit durchlässiger Front. HANSA, Zentralorgan für Schifffahrt, Schiffbau, Hafen, Vol. 139, 7, 2002.
- BERGMANN, H. and OUMERACI, H.: Wave-induced water levels and pressure distribution at perforated wall. Proc. 7th International Conference on Coastal and Port Engineering in Developing Countries (PIANC COPEDEC VII, Dubai, UAE), 2008.
- D'ELISO, C.; OUMERACI, H. and KORTENHAUS, A.: A model system for breaching of sea dikes. Proc. International Conference on Coastal Structures '07 (CSt, Venice, Italy), 2007.
- DETTE, H.; PETERS, K. and NEWE, J.: Large Wave Flume experiments '96/97 on equilibrium profiles with different beach slopes. LWI Report, 825, TU Braunschweig, 1998a.
- DETTE, H.; PETERS, K. and NEWE, J.: Large Wave Flume experiments '96/97 on beach and dune stability. LWI Report, 830, TU Braunschweig, 1998b.
- EAK: Empfehlungen des Ausschusses für Küstenschutzwerke. Ausschuss für Küstenschutzwerke der Deutschen Gesellschaft für Erd- und Grundbau e.V. und der Hafenbautechnischen Gesellschaft e.V. Die Küste 65, 2002.
- FÜHRBÖTER, A.; SPARBOOM, U. and WITTE, H.-H.: Großer Wellenkanal Hannover: Versuchsergebnisse über den Wellenaufbau auf glatten und rauhen Deichböschungen mit der Neigung 1 : 6. Die Küste 50, 1989.
- GEISENHAINER, P. and OUMERACI, H.: Large-scale experiments on dike-breaching and breach growth. Proc. International Conference on Coastal Structures (CSt, Venice, Italy), 2007.
- GEISENHAINER, P. and OUMERACI, H.: Large-scale experiments on dike breaching and breach growth. Proc. 31st International Conference on Coastal Engineering (ICCE, Hamburg, Germany), 2008.
- GL-GUIDELINES: Guidelines for the certification of offshore wind turbines. German Lloyds, Hamburg, 2005.
- GRÜNE, J. and FÜHRBÖTER, A.: Large Wave Channel for “full-scale modelling” of Wave Dynamics in Surf Zones. Proc. Symposium on Modelling Techniques, San Francisco, USA, Vol. I, 1975.
- HAYAKAWA, T.; KIMURA, K.; TAKAHASHI, S.; MUTTRAY, M.; KUDELLA, M. and OUMERACI, H.: Wave splash height on a high-mound composite breakwater. Proc. 4th International Conference on Hydrodynamics (ICHHD, Yokohama, Japan), Vol. 2, 2000.

- HILDEBRANDT, A.: Seegangsbelastung schlanker lotrechter Pfähle in Gruppenanordnungen. Graduate Thesis, TU Braunschweig, FZK, Bergische Universität Wuppertal (unpublished), 2006.
- HILDEBRANDT, A.; SPARBOOM, U. and OUMERACI, H.: Wave forces on group of slender cylinders in comparison to an isolated cylinder due to non-breaking waves. Proc. 31st International Conference on Coastal Engineering (ICCE, Hamburg, Germany), 2008.
- HUGHES, S.: Physical models and laboratory model techniques in coastal engineering, World Scientific Publishing, 1993.
- IRSCHIK, K.: Belastung von zylindrischen Pfahlstrukturen durch brechende und nicht brechende Wellen. PhD thesis to be submitted to TU Braunschweig, 2012.
- IRSCHIK, K.; OUMERACI, H. and SCHIMMELS, S.: Breaking criteria for laboratory experiments based on the Phase-Time Method (PTM). Proc. 32nd International Conference Coastal Engineering (ICCE, Shanghai, China), 2010.
- IRSCHIK, K.; SPARBOOM, U. and OUMERACI, H.: Breaking Wave Characteristics for the Loading of a Slender Pile. Proc. 28th International Conference on Coastal Engineering (ICCE, Auckland, New Zealand), 2002.
- IRSCHIK, K.; SPARBOOM, U. and OUMERACI, H.: Breaking Wave Loads on a Slender Pile in Shallow Water. Proc. 29th International Conference on Coastal Engineering (ICCE, Cardiff, UK), 2004.
- ISO/IEC: Design requirements for offshore wind turbines. ISO/IEC 61400-3, 2009.
- ISO: Actions from wave and currents on marine structures. ISO 21650, 2007.
- JULIFS, J.: Breaking wave loads on a vertical slender cylinder within a cylinder group. Student project report, TU Braunschweig (unpublished), 2006.
- KIMURA, K.; FUJIKI, T.; KAMIKUBO, K.; ABE, R. and ISHIMOTO, K.: Damages to vehicles on a coastal highway by wave action. Proc. International Conference on Coastal Structures '99 (CSt, Santander, Spain), Vol. 2, 2000.
- KOETHER, G.: Hydraulische Wirksamkeit getauchter Einzelfilter und Filtersysteme – Prozessbeschreibung und Modellbildung für ein innovatives Riffkonzept. PhD thesis, TU Braunschweig, LWI, 2002.
- KOETHER, G.; BERGMANN, H. and OUMERACI, H.: Wave attenuation by submerged filter systems. Proc. 4th International Conference on Hydrodynamics (ICHHD, Yokosuka, Japan), Vol. 2, 2000.
- KOETHER, G. and OUMERACI, H.: Schutzbauwerke für Sandstrände mit touristischer und ökologischer Bedeutung – Unterwasser-Filtersysteme, HANSA, Zentralorgan für Schifffahrt, Schiffbau, Hafen, Vol. 138, 11, 2001.
- KORTENHAUS, A. and OUMERACI, H.: Scale effects in modelling wave impact loading of coastal structures. Proc. Hydralab workshop on “Experimental research and its synergy effects with mathematical models”, Hannover, Germany, 2003.
- KUDELLA, M. and OUMERACI, H.: Wave-Induced Pore Pressure in the Sandy Seabed Underneath a Caisson Breakwater – Experimental Results of Large Scale Model Tests. Technical Report, TU Braunschweig, LWI, 2004.
- KUDELLA, M. and OUMERACI, H.: Pore pressure development in the sand bed underneath a caisson breakwater. Proc. 24th International Conference on Coastal Engineering 2004 (Lisbon, Portugal), Vol. 4, World Scientific, 2005.
- KUDELLA, M.; OUMERACI, H.; DE GROOT, M. B. and MEIJERS, P.: Large-scale experiments on pore pressure generation underneath a caisson. Journal of Waterway, Port, Coastal and Ocean Engineering, Vol. 132, 4, 2006.
- LE MEHAUTÉ, B.: Wave absorbers in harbours. Report no. 2–122, US Army Waterways Experiment Station, Vicksburg, USA, 1965.
- MORI, M.; YAMAMOTO, Y. and KIMURA, K.: Wave force and stability of upright section of high mound composite seawall. Proc. 31st International Conference on Coastal Engineering (ICCE, Hamburg, Germany), 2008.
- MUTTRAY, M.: Wave motion at and in rubble mound breakwaters-large-scale model and theoretical investigation, PhD thesis, TU Braunschweig, LWI, 2000.
- MUTTRAY, M. and OUMERACI, H.: Theoretical and experimental study on wave damping inside a rubble mound breakwater. Coastal Engineering, Vol. 52, 8, 2005.
- MUTTRAY, M.; OUMERACI, H.; SHIMOSAKO, K. and TAKAHASHI, S.: Hydraulic performance of high mound composite breakwater. Proc. 26th International Conference on Coastal Engineering (ICCE, Copenhagen, Denmark), 1998.

- MUTTRAY, M.; OUMERACI, H.; SHIMOSAKO, K. and TAKAHASHI, S.: Wave load on an innovative high mound composite breakwater: Results of large scale experiments and tentative design formulae. Proc. Conference on Coastal Structures '99 (CSt, Santander, Spain), Vol. 1, 2000.
- NEWE, J.: Methodik für großmaßstäbliche 2D-Experimente zum Strandverhalten unter Sturmflutbedingungen. PhD thesis, LWI, TU Braunschweig, 2002.
- NEWE, J.: Beach profile development under storm waves – Methodology for large-scale model testing and prediction formulae. Extended summary of PhD thesis, TU Braunschweig, LWI, 154, 2006.
- NICKELS, H. and HEERTEN, G.: Objektschutz Haus Kliffende. HANSA Zentralorgan für Schifffahrt, Schiffbau, Hafen, Vol. 137, 3, 2000.
- OUMERACI, H.: Scale effects in coastal hydraulic modelling. Proc. International Association for Hydro-Environment Engineering and Research (IAHR) Symposium on scale effects in modelling hydraulic structures (Esslingen, Germany), 1984.
- OUMERACI, H.: Scour in front of vertical breakwaters. Review of scaling problems. Proc. International Workshop on wave barriers in deep water. Port and Harbour Research Institute (Yokosuka, Japan), 1994a.
- OUMERACI, H.: Review and analysis of vertical breakwater failures: Lessons learned. Coastal Engineering. Special Issue on Vertical Breakwaters, Vol. 22 (1/2), 1994b.
- OUMERACI, H.: Forschungszentrum Küste (FZK). HANSA – Schifffahrt – Schiffbau – Hafen, Vol. 135, 6, pp. 63–67, 1998.
- OUMERACI, H.: Strengths and limitations of physical modelling in coastal engineering. In Evers, K.V. et al. (eds.), Proc. of Hydralab workshop on “Experimental research and its synergy effects with mathematical models”, Hannover, Germany, 1999.
- OUMERACI, H.: The sustainability challenge in coastal engineering. In Goda, Y. et al. (eds.), Keynote Lecture. Proc. 4th International Conference on Hydrodynamics (ICHD, Yokohama, Japan), Vol. 1, 2000.
- OUMERACI, H.: Breakwaters Part 2. In Agerschou, H. (ed.), Planning and design of ports and marine terminals, London, UK: Thomas Telford, 2004.
- OUMERACI, H.: Nearshore and Onshore tsunami effects. Background for DFG-Round Table Discussion, Hannover, 2006.
- OUMERACI, H.: Nonconventional wave damping structures. In Young C. Kim (ed.), Invited Chapter in Handbook of Coastal and Ocean Engineering, World Scientific, 2010a.
- OUMERACI, H.: Composite modelling in Coastal Engineering. Report HYDRALAB III, 2010b.
- OUMERACI, H.: Dimensional analysis, physical modelling and scaling. Chapter for Guidelines in ecological modelling. Hydralab IV (planned for publication by IAHR), 2010c.
- OUMERACI, H.; BLECK, M.; HINZ, M. and KÜBLER, S.: Large-scale model test for hydraulic stability of geotextile sand containers under wave attack. LWI Report, 878, 2002.
- OUMERACI, H.; CLAUSS, G. F.; HABEL, R. and KOETHER, G.: Unterwasser Filtersysteme zur Wellendämpfung. Final Report of BMBF-Research Project, 2001a.
- OUMERACI, H.; GRÜNE, J.; SPARBOOM, U.; SCHMIDT-KOPPENHAGEN, R. and WANG, Z.: Large-scale model investigation of scour development and scour protection for monopile foundations of offshore wind turbine in the North Sea. Final Report. Coastal Research Centre (FZK), Hannover, 2000a.
- OUMERACI, H.; HINZ, M.; BLECK, M. and KORTENHAUS, A.: Sand-filled geotextile containers for shore protection. Proc. 6th International Conference on Coastal and Port Engineering in Developing Countries (COPEDEC, Colombo, Sri Lanka), 2003.
- OUMERACI, H. and KOETHER, G.: Hydraulic performance of a submerged wave absorber for coastal protection. Advances in Coastal and Ocean Engineering, World Scientific, 2009.
- OUMERACI, H.; KORTENHAUS, A.; ALLSOP, N. W. H.; DE GROOT, M. B.; CROUCH, R. S., VRIJLING, J. K. and VOORTMAN, H. G.: Probabilistic design tools for vertical breakwaters. Balkema, 2001b.
- OUMERACI, H.; KORTENHAUS, A.; BREUSTEDT, H. and SCHLEY, P.: Hydraulic model investigations on breakwaters with a core made of geotextile sand containers. Report 933, LWI, TU Braunschweig, 2007.
- OUMERACI, H.; KUDELLA, M.; MUTTRAY, M.; KIMURA, K. and HAYAKAWA, T.: Wave runup and wave overtopping on a high mound composite breakwater. Final Report, 831, LWI, TU Braunschweig, 1998.

- OUMERACI, H.; KUDELLA, M. and STAAL, T.: Pre-design and preparatory works for the large-scale model tests on ELASTOCOAST revetment in GWK. Research Report no. 986, LWI, TU Braunschweig, 2009a.
- OUMERACI, H. and MUTTRAY, M.: Large scale model tests on a high-mound composite type breakwater. Research Report 818, LWI, TU Braunschweig, 1997.
- OUMERACI, H.; MUTTRAY, M.; KUDELLA, M.; KIMURA, K. and TAKAHASHI, S.: Wave loading of a high mound composite breakwater (HMCB) with splash reducers. Proc. 4th International Conference on Hydrodynamics (ICHHD, Yokohama, Japan), Vol. 2, 2000b.
- OUMERACI, H. and PARTENSKY, H. W.: Wave-induced pore pressure in rubble mound breakwaters – Results and data from large-scale model tests. Research Report, TPB3/91/01, FI, LU Hannover, 1991.
- OUMERACI, H. and RECIO, J.: Geotextile sand containers for shore protection. In Young C. Kim (ed.), Invited chapter in Handbook of Coastal and Ocean Engineering, World Scientific, 2010.
- OUMERACI, H.; SCHÜTTRUMPF, H.; KORTENHAUS, A.; KUDELLA, M.; MÖLLER, J. and MUTTRAY, M.: Untersuchungen zur Erweiterung bzw. zum Umbau des Deckwerks am Nordstrand von Norderney. Research Report 853, LWI, TU Braunschweig, 2000c.
- OUMERACI, H.; STAAL, T.; PFOERTNER, S. and LUDWIGS, G.: Hydraulic performance, wave loads and response of ELASTOCOAST revetments and their foundation. Keynote lecture. Proc. Journées Nationales du Génie Civil & Génie Cotier (Sables d'Olonne, France), 2010a.
- OUMERACI, H.; STAAL, T.; PFOERTNER, S. and LUDWIGS, G.: Hydraulic performance, wave loads and response of PBA revetments and their foundation. European Journal of Civil and Environmental Engineering (in press), 2011.
- OUMERACI, H.; STAAL, T.; PFOERTNER, S.; LUDWIGS, G. and KUDELLA, M.: Hydraulic performance, wave loads and response of ELASTOCOAST revetments and their foundation – A large scale model study. Final Report, Report 988, LWI, TU Braunschweig, 2009b.
- OUMERACI, H.; STAAL, T.; PFOERTNER, S.; KUDELLA, M.; SCHIMMELS, S. and VERHAGEN, H. H.: Hydraulic Performance Of Elastomeric Bonded Permeable Revetments And Subsoil Response To Wave Loads. Proc. 32nd International Conference on Coastal Engineering (ICCE, Shanghai, China), 2010b.
- PETERS, K.: Morphodynamics of sandy coast in the surf zone – Suspended load. PhD thesis, LWI Report 146, TU Braunschweig, 2000.
- PREPERNAU, U.; GRÜNE, J.; SPARBOOM, U.; SCHMIDT-KOPPENHAGEN, R.; WANG, Z. and OUMERACI, H.: Large-scale model study on scour around slender monopile induced by irregular waves. Proc. International Conference on Coastal Engineering (ICCE, Germany, Hamburg), 2008a.
- PREPERNAU, U.; GRÜNE, J. and OUMERACI, H.: Evaluation on composite modelling of piles and spheres – Task 5: Scour around vertical slender monopoles. Report HYDRALAB III, 2009.
- PREPERNAU, U.; GRÜNE, J.; SCHMIDT-KOPPENHAGEN, R.; WANG, Z. and OUMERACI, H.: Large-scale model tests on scour around slender monopile under live-bed conditions. Proc. Coastlab Conference (Italia, Bari), 2008b.
- RECIO, J. and OUMERACI, H.: Effect of deformations on the hydraulic stability of coastal structures made of geotextile sand containers. Journal of Geotextiles and Geomembranes, Vol. 25, 2007.
- RECIO, J. and OUMERACI, H.: Hydraulic permeability of GSC-structures: Laboratory results and conceptual model. Journal of Geotextiles and Geomembranes, 2008.
- RECIO, J. and OUMERACI, H.: New stability formulae for coastal structures made of geotextile sand containers. Coastal Engineering, Elsevier, 2009a.
- RECIO, J. and OUMERACI, H.: Processes affecting the hydraulic stability of GSC structures: experimental and numerical. Coastal Engineering, Elsevier, 2009b.
- SAATHOFF, F.; OUMERACI, H. and RESTALL, S.: Australian and German experiences on the use of geotextile containers. Journal of Geotextiles and Geomembranes, Vol. 25, 2007.
- SCHMIDT-KOPPENHAGEN, R., OUMERACI, H., GRÜNE, J., SPARBOOM, U. and WIENKE, J.: Freak-Wave Generation in the Large Wave Channel of Hannover. 1st EGU General Assembly-Natural Hazards, Poster no. EGU 04-A-02885, European Geosciences Union (EGU), 2004.

- SCHÜTTRUMPF, H.: Wellenüberlaufströmung bei Seedeichen. PhD thesis, TU Braunschweig, LWI, 2001.
- SCHÜTTRUMPF, H.; OUMERACI, H.; KIMURA, K.; HAYAKAWA, T. and MOELLER, J.: Wave overtopping on a high mound composite breakwater. Proc. International Conference on Coastal Structures '99 (CSt, Santander, Spain), Vol. 1, 2000.
- SCHÜTTRUMPF, H.; OUMERACI, H.; THORENZ, F. and MÖLLER, J.: Reconstruction and rehabilitation of a historical seawall at Norderney. In: Allsop, N. W. H. (ed.), ICE, Proc. Breakwaters, Coastal Structures and Coastlines, Thomas Telford (London, UK), 2002.
- SPARBOOM, U.: Naturmaßstäbliche Untersuchungen an Deckwerken im Großen Wellenkanal. Symp. „Deckwerke“ am 8. und 9.6.1988, Karlsruhe. Mitteilungsblatt der Bundesanstalt für Wasserbau, 66, 1988.
- SPARBOOM, U. and OUMERACI, H.: Wave loads on slender marine cylinders depending on the interaction effects of adjacent cylinders. Proc. 25th International Conference on Ocean, Offshore and Arctic Engineering (OMAE, Hamburg, Germany), 2006.
- STANCZAK, G. and OUMERACI, H.: Modeling sea dike breaching induced by breaking wave impact-laboratory experiments and computational model. Coastal Engineering, Elsevier, Vol. 59, 1, 2012.
- TAKAHASHI, S.; SHIMOSAKO, K.; OUMERACI, H.; MUTTRAY, M. and KIMURA, K.: Reduced wave overtopping characteristics of a new high mound composite breakwater: results of small-scale experiments. Proc. Conference on Coastal Structures '99 (CSt, Santander, Spain), Vol. 1, 2000.
- TUAN, T. Q. and OUMERACI, H.: A numerical model for wave overtopping of seadikes. Coastal Engineering, Vol. 57, 8, Elsevier, 2010.
- TUAN, T. Q. and OUMERACI, H.: Numerical modelling of wave overtopping induced erosion of grassed inner dike slopes seadikes. Natural Hazards (submitted), 2011.
- WIENKE, J.: Druckschlagbelastung auf schlanke zylindrische Bauwerke durch brechende Wellen. Theoretische und großmaßstäbliche Laboruntersuchungen. PhD thesis, TU Braunschweig, 2001.
- WIENKE, J. and OUMERACI, H.: Breaking wave impact force on a vertical and inclined slender pile – Theoretical and large-scale investigations. Coastal Engineering, Vol. 52, 2005.
- WOUTERS, J.: Slope revetment – Stability of geosystems. Delft Hydraulics Report, 1998.